

Stochastic Schrödinger equation approach to real-time dynamics of Anderson-Holstein impurities: an open quantum system perspective

Zhen Huang,¹ Limin Xu,² and Zhennan Zhou^{3,*}

¹*Department of Mathematics, University of California, Berkeley, CA 94720, USA*

²*Department of Mathematical Sciences, Tsinghua University, Beijing 100084, China*

³*Beijing International Center for Mathematical Research, Peking University, Beijing, 100871, China*

We develop a stochastic Schrödinger equation (SSE) framework to simulate real-time dynamics of Anderson-Holstein (AH) impurities coupled to a continuous fermionic bath. The bath degrees of freedom are incorporated through fluctuating terms determined by exact system-bath correlations, which is derived in an *ab initio* manner. We show that such an SSE treatment provides a middle ground between numerically expansive microscopic simulations and macroscopic master equations. Computationally, the SSE model enables efficient numerical methods for propagating stochastic trajectories. We demonstrate that this approach not only naturally provides microscopically-detailed information unavailable from reduced models, but also captures effects beyond master equations, thus serves as a promising tool to study open quantum dynamics emerging in physics and chemistry.

I. INTRODUCTION

Real-time dynamics of quantum impurity systems with fermionic baths have been a central topic in condensed matter physics for the past few decades. It is used to model a wide range of systems, such as magnetic impurities in metals [1], quantum dot systems [2], atom adsorption onto surface [3]. Among various types of quantum impurity models, the Anderson-Holstein (AH) model [4, 5] is of critical importance, since it is directly related to chemisorption [4], electrochemistry [6], heterogeneous catalysis [7] and molecular junctions [8].

The Anderson-Holstein model comprises of a molecular system as the impurity part and the continuous heat bath equilibrated at a certain temperature as the environment. For example, when modeling molecule-metal interfaces, the bath part is made up of metal orbitals of a continuum of spectra [4, 5]. The most straightforward simulation strategy would be a direct discretization of the bath orbitals (for example, see [9, 10]), and then propagate the many-body Schrödinger equation for the entire extended system. However, such calculations are often so expensive that either one is only capable of studying a model with a very small number of bath orbitals [11], or one makes crude single-particle approximations [12]. These treatments are far from exact and are only effective in limited scenarios.

The impurities could be viewed as a fermionic open quantum system due to the influence of the infinite bath. To incorporate the open-system effects with a manageable computational cost, various master equations are developed based on different physical approximations. This is generally seen in the study of molecular-metal interfaces. Treating the nuclei of the molecular system as classical particles, classical master equations (CME) [13, 14] are proposed along with surface hopping technique [15, 16] to efficiently sample the ensemble at equilibrium.

However, due to the breakdown of the Born-Oppenheimer approximation, it is necessary to capture the nuclear quantum effects and nonadiabatic dynamics simultaneously. This is often achieved by quantum master equations (QME), which describe the dynamics for the reduced density matrix by tracing out the electronic degree of freedom. Lindblad master equations [17, 18] are used when one makes the Markovian approximation. To capture the memory effects, Nakajima-Mori-Zwanzig equations [19, 20], Redfield equations [21, 22] and other non-Markovian equations [23–25] are proposed as effective models. QME is widely used to model realistic systems [24–27]. The hierarchy quantum master equation (HQME) [27–29], also known as the hierarchy equation of motion (HEOM), is a nonperturbative alternative but is often computationally too expensive.

However, there is another widely-used approach, namely Stochastic Schrödinger equations (SSE), for studying open quantum systems. By incorporating stochastic fluctuations arising from interactions with the external environment, SSE has been successfully used in modeling quantum decoherence [30, 31], quantum measurement [32–34], quantum jumps [35, 36] and so on. It is found to be consistent with QME calculations in many cases [37–40], and in the meantime has the following additional advantages: on the one hand, SSE provides an ensemble of time-dependent quantum trajectories, and therefore is very convenient for studying the statistical and nonequilibrium properties of the open system; on the other hand, the numerical methods for simulating stochastic differential equations have already been studied extensively [41, 42], and as a result the above trajectories could be obtained effectively with a Monte-Carlo sampling scheme. However, the success of SSE models highly relies on the accurate modeling of the environment, i.e. obtaining the exact time-correlation function of the noise term in SSE.

Even though SSE is a very powerful tool in the modeling of open quantum systems, it has not been applied to study the real-time dynamics of quantum impurities

* zhennan@bicmr.pku.edu.cn

with fermionic bath, to the best of our knowledge. On the one hand, SSE approaches are mostly developed for bosonic heat bath in different regimes. On the other hand, although there are attempts of using SSE to study fermionic bath effects [37, 43], there lacks an ab initio treatment of the stochastic and non-Markovian effects, therefore not applicable to general chemical systems such as molecule-metal interfaces.

The purpose of this article is two-fold. On the one hand, we aim to fill in a gap in the study of Anderson-Holstein models as an open quantum system: the time-correlation function of the noise term in SSE is obtained directly from the Anderson-Holstein Hamiltonian. On the other hand, we emphasize the following hierarchy of modeling: SSE is at an intermediate level of approximation, right between the atomic-level AH model and the QME model:

$$\text{Anderson-Holstein} \rightarrow \text{SSE} \rightarrow \text{QME}.$$

For a detailed description of this modeling hierarchy, please see Fig. 1. Although every SSE is associated with a corresponding QME, SSEs are able to encapsulate many intricate microscopic details, while QMEs merely describe the statistical averages of the SSE trajectories. This is also seen in our numerical experiments Section V. In other words, QME should be viewed as a further approximation on top of SSE.

The rest of this article is organized as follows. In Section II, we derive the stochastic Schrödinger equations from the Anderson-Holstein model. After introducing the problem setup in Section II.1, we review the Bogoliubov transformation in Section II.2, and then derive the time correlation function in Section II.3. We finally arrive at the non-Markovian SSE model in Section II.4 and its wide band limit in Section II.5. In Section III.1, we discuss how to obtain quantum master equations from SSE by taking expectation values of density matrices. In Section III.2, we show how different approximations would lead to different versions of QME, and demonstrate the hierarchy of modeling in detail. In Section IV, we discuss the numerical methods for trajectory-based SSE simulations. We introduce how to generate time-correlated noise in Section IV.1, and how to do time evolution in Section IV.2. We show numerical experiments in Section V. We demonstrate that SSE offers directly an ensemble of particle trajectories with microscopic details, and compare its results to QME.

II. FROM AH MODEL TO SSE

II.1. Setup

In the Anderson-Holstein model [5], the total Hamiltonian consists of three parts: the system Hamiltonian \hat{H}_S , the bath Hamiltonian \hat{H}_B , and the system-bath in-

teraction $\lambda\hat{H}_{S-B}$:

$$\hat{H} = \hat{H}_S + \hat{H}_B + \lambda\hat{H}_{S-B}. \quad (1)$$

Here \hat{H}_S is the system Hamiltonian, \hat{H}_B is the bath Hamiltonian, and $\lambda\hat{H}_{S-B}$ is the Hamiltonian of the interaction between the system and bath where λ is the interaction strength. The system Hamiltonian \hat{H}_S consists of the kinetic and potential energy of the nuclei:

$$\hat{H}_S = \frac{\hat{p}^2}{2m_n} + U_0(\hat{x}) + h(\hat{x})\hat{d}^\dagger\hat{d}, \quad (2)$$

where \hat{p} and \hat{x} are the momentum operator and the position operator for the nuclei, m_n is the mass of the nuclei, \hat{d} and \hat{d}^\dagger are the fermionic annihilation and creation operators corresponding to the ground state electronic orbital. Here we are considering a two-level nuclei: when the molecule is neutral, $\hat{d}^\dagger\hat{d} = 0$, and the nuclear potential is $U_0(\hat{x})$; when the molecule is charged, $\hat{d}^\dagger\hat{d} = 1$, and the potential is $U_1(x) = U_0(\hat{x}) + h(\hat{x})$.

The system's Hamiltonian represents a two-level electronic system and therefore could be rewritten in the following matrix form:

$$\begin{aligned} \hat{H}_S &= \begin{pmatrix} \hat{h}_0(x) & \\ & \hat{h}_1(x) \end{pmatrix} \\ &= \begin{pmatrix} -\frac{\varepsilon^2}{2}\Delta + U_0(x) & \\ & -\frac{\varepsilon^2}{2}\Delta + U_1(x) \end{pmatrix}. \end{aligned} \quad (3)$$

Here ε is the ratio between the energy scale we are interested in and the macroscopic energy scale, which is a moderately small non-dimensionalized constant but fixed in the derivation, and it is also known as the semiclassical parameter [44]. The system wavefunction is

$$\psi(x) = \begin{pmatrix} \psi_0(x) \\ \psi_1(x) \end{pmatrix} \in \mathbb{L}^2(\mathbb{R}^n) \otimes \mathbb{C}^2,$$

where $\psi_0(x)$ is the nuclei wavefunction when the molecule is neutral (i.e. under potential $U_0(x)$), while $\psi_1(x)$ is the nuclei wavefunction when the molecule is charged (i.e. under potential $U_1(x)$). We also introduce the following Dirac notation, as it is widely used in literature:

$$|\Psi\rangle = |\Psi_0\rangle|0\rangle + |\Psi_1\rangle|1\rangle,$$

and in this notation, \hat{d} and \hat{d}^\dagger acts as $\hat{d}|1\rangle = |0\rangle$, $\hat{d}^\dagger|0\rangle = |1\rangle$, $\hat{d}|0\rangle = 0$, $\hat{d}^\dagger|1\rangle = 0$, and we have

$$\begin{aligned} \hat{d}|\Psi\rangle &= \hat{d}|\Psi_0\rangle|0\rangle + \hat{d}|\Psi_1\rangle|1\rangle = |\Psi_1\rangle|0\rangle \\ \hat{d}^\dagger|\Psi\rangle &= \hat{d}^\dagger|\Psi_0\rangle|0\rangle + \hat{d}^\dagger|\Psi_1\rangle|1\rangle = |\Psi_0\rangle|1\rangle. \end{aligned} \quad (4)$$

In Eq. (4), when acting on $|\Psi\rangle \in \mathbb{L}^2(\mathbb{R}^n) \otimes \mathbb{C}^2$, \hat{d} acts as $\hat{I} \otimes \hat{d}$ (so is \hat{d}^\dagger).

The heat bath is formed by non-interacting metal orbitals $|E\rangle$ with energy $E \in [E_-, E_+]$, where E_- and E_+

are the lower and upper bound of the spectrum of the metal continuum band. As a result, the bath Hamiltonian is

$$\hat{H}_B = \int_{E_-}^{E_+} (E - \mu) \hat{c}_E^\dagger \hat{c}_E dE. \quad (5)$$

Here \hat{c}_E and \hat{c}_E^\dagger are the annihilation and creation operators for the metal electronic orbital $|E\rangle$, and μ is the chemical potential. For formal simplicity, μ is chosen to be zero unless otherwise specified, but all of our derivations naturally apply to any choice of μ . For the sake of practical calculations, the continuous band $[E_-, E_+]$ could be discretized using equidistant grid point [10]:

$$E_k = E_- + (k - \frac{1}{2})h_N, \quad h_N = \frac{E_+ - E_-}{N}. \quad (6)$$

or using Gaussian quadrature [9]. After discretization, the bath Hamiltonian becomes:

$$\hat{H}_B = \sum_{k=1}^N E_k \hat{c}_k^\dagger \hat{c}_k. \quad (7)$$

For now, we will proceed our discussion using the discretized metal orbitals. However, as we will show later, after deriving the nMSSE model, we will consider the continuous band limit by letting the number of metal orbitals N go to infinity, through which we recover the metal continuum and thus eliminate the quadrature error of continuous band discretization.

The system-bath interaction \hat{H}_{S-B} , which describes the interaction between the molecule and metal continuum, is as follows:

$$\lambda \hat{H}_{S-B} = \lambda \left(\int dE V(E, \hat{x}) \hat{c}_E^\dagger \hat{d} + \bar{V}(E, \hat{x}) \hat{d}^\dagger \hat{c}_E \right). \quad (8)$$

Here $V(E, x)$ describes the interaction strength between the molecule and the bath orbital with energy E while the nuclei is at x , and $\bar{V}(E, x)$ is its complex conjugate. With the same discretization orbitals $\{E_k\}_{k=1}^N$ chosen as above, we have

$$\lambda \hat{H}_{S-B} = \lambda \left(\sum_{k=1}^N V_k(\hat{x}) \hat{c}_k^\dagger \hat{d} + \bar{V}_k(\hat{x}) \hat{d}^\dagger \hat{c}_k \right) \quad (9)$$

where $V_k(\hat{x}) = \sqrt{h_N} V(E, x)$. We refer to [9] for the derivation of Eq. (9). Without loss of generality, let us assume that $V_k(x)$ is real-valued.

II.2. Bogoliubov transformation of the system-bath coupling

For clarity in the derivation, we adopt the Bogoliubov transformations, which were introduced for studying weakly interacting He^4 superfluid [45] and solving

Bardeen–Cooper–Schrieffer theory [46] to understand superconductivity. Let us define the following pairs of Bogoliubov operators:

$$\begin{aligned} \hat{B}_{1k} &= \hat{c}_k + \hat{c}_k^\dagger, & \hat{B}_{2k} &= i(\hat{c}_k - \hat{c}_k^\dagger), \\ \hat{g}_1 &= \hat{d} + \hat{d}^\dagger, & \hat{g}_2 &= i(\hat{d} - \hat{d}^\dagger). \end{aligned} \quad (10)$$

Note that $\hat{B}_{1k}, \hat{B}_{2k}, \hat{g}_1, \hat{g}_2$ are all Hermitian operators, and we have

$$\begin{aligned} \hat{c}_k &= \frac{\hat{B}_{1k} - i\hat{B}_{2k}}{2}, & \hat{c}_k^\dagger &= \frac{\hat{B}_{1k} + i\hat{B}_{2k}}{2} \\ \hat{d} &= \frac{\hat{g}_1 - i\hat{g}_2}{2}, & \hat{d}^\dagger &= \frac{\hat{g}_1 + i\hat{g}_2}{2}. \end{aligned} \quad (11)$$

In Dirac's notation, according to Eq. (4), we have

$$\begin{aligned} \hat{g}_1 |\Psi\rangle &= (\hat{d} + \hat{d}^\dagger)(|\psi_0\rangle|0\rangle + |\psi_1\rangle|1\rangle) \\ &= |\psi_0\rangle|1\rangle + |\psi_1\rangle|0\rangle, \\ \hat{g}_2 |\Psi\rangle &= i(\hat{d} - \hat{d}^\dagger)(|\psi_0\rangle|0\rangle + |\psi_1\rangle|1\rangle) \\ &= -i|\psi_0\rangle|1\rangle + i|\psi_1\rangle|0\rangle. \end{aligned} \quad (12)$$

Therefore the Bogoliubov operators \hat{g}_1, \hat{g}_2 acts like Pauli matrices for the two-level system:

$$\hat{g}_1 = \sigma_x = \begin{pmatrix} 0 & 1 \\ 1 & 0 \end{pmatrix}, \quad \hat{g}_2 = -\sigma_y = \begin{pmatrix} 0 & i \\ -i & 0 \end{pmatrix}. \quad (13)$$

Note that $[B_{ik}, g_j]_+ = 0$, we can rewrite the coupling Hamiltonian as:

$$\begin{aligned} \hat{H}_{S-B} &= \sum_{k=1}^N V_k \left(\frac{\hat{B}_{1k} + i\hat{B}_{2k}}{2} \frac{\hat{g}_1 - i\hat{g}_2}{2} + \frac{\hat{g}_1 + i\hat{g}_2}{2} \frac{\hat{B}_{1k} - i\hat{B}_{2k}}{2} \right) \\ &= \sum_{k=1}^N V_k \left(\frac{\hat{g}_1 + i\hat{g}_2}{2} \frac{\hat{B}_{1k} - i\hat{B}_{2k}}{2} - \frac{\hat{g}_1 - i\hat{g}_2}{2} \frac{\hat{B}_{1k} + i\hat{B}_{2k}}{2} \right) \\ &= \sum_{k=1}^N \frac{i}{2} V_k(x) \hat{g}_2 \hat{B}_{1k} - \frac{i}{2} V_k(x) \hat{g}_1 \hat{B}_{2k}. \end{aligned} \quad (14)$$

In open quantum systems, the system-bath interaction is often written as a sum of multiplication of system Hermitian operator and bath Hermitian operator:

$$\hat{H}_{S-B} = \sum_{i=1}^2 \sum_{k=1}^N \hat{S}_{ik} \hat{B}_{ik}. \quad (15)$$

Combined with Eq. (14), we know that the system operators \hat{S}_{ik} are

$$\hat{S}_{1k} = \frac{i}{2} V_k(x) \hat{g}_2, \quad \hat{S}_{2k} = -\frac{i}{2} V_k(x) \hat{g}_1. \quad (16)$$

II.3. Time correlation function of bath operators and the memory kernel

The non-Markovian Stochastic Schrödinger Equation (nMSSE) was formally derived in [47] and was applied to

simulate spin-boson systems. For a general open quantum system where the interaction between system and bath is described as $\hat{H}_{S-B} = \sum_{\alpha} \hat{S}_{\alpha} \hat{B}_{\alpha}$, the effective nMSSE dynamics for the system is

$$\begin{aligned} i\varepsilon \partial_t |\Psi(t)\rangle &= \hat{H}_S |\Psi(t)\rangle + \lambda \sum_{\alpha} \eta_{\alpha}(t) \hat{S}_{\alpha} |\Psi(t)\rangle \\ &- i \frac{\lambda^2}{\varepsilon} \int_0^t d\tau \sum_{\alpha, \beta} C_{\alpha, \beta}(\tau) \hat{S}_{\alpha} e^{-\frac{i}{\varepsilon} \hat{H}_S \tau} \hat{S}_{\beta} |\Psi(t-\tau)\rangle. \end{aligned} \quad (17)$$

Recall that ε is a small non-dimensionalized parameter. Here $\eta_{\alpha}(t)$ is the complex-valued Gaussian stochastic noise satisfying

$$\begin{aligned} \mathbb{E}(\eta_{\alpha}(t)) &= 0, \quad \mathbb{E}(\eta_{\alpha}(t)\eta_{\beta}(t')) = 0, \\ \mathbb{E}(\eta_{\alpha}^*(t)\eta_{\beta}(t')) &= C_{\alpha, \beta}(t-t'), \end{aligned} \quad (18)$$

and the memory kernel $C_{\alpha, \beta}(\tau)$ is the time-correlation function of the bath operators:

$$C_{\alpha, \beta}(t-t') = \text{tr}_B \left(\hat{\rho}_B^{\text{eq}} \hat{B}_{\alpha}(t) \hat{B}_{\beta}(t') \right), \quad (19)$$

where $\hat{\rho}_B^{\text{eq}} = \frac{1}{Z_B} \exp(-\beta \hat{H}_B) = \frac{1}{Z_B} \exp(-\hat{H}_B/k_B T)$ is the density matrix of the bath, which is in thermal equilibrium of temperature T , k_B is the Boltzmann constant, $Z_B = \text{tr}(\exp(-\hat{H}_B/k_B T))$ and $\hat{B}_{\alpha}(t) = \exp(\frac{i}{\varepsilon} \hat{H}_B t) \hat{B}_{\alpha} \exp(-\frac{i}{\varepsilon} \hat{H}_B t)$ is the Heisenberg representation of \hat{B}_{α} . In other words, the derivation of SSE model for Anderson-Holstein impurities boils down to calculating the time-correlation function Eq. (19) of the stochastic noise, which is also the memory kernel of the non-Markovian term.

Now let us derive an explicit expression for Eq. (19). Recall that N is the number of discrete metal bath orbitals. The natural basis for the Fock space \mathcal{H}_B of the bath, under the occupation number representation, would be

$$\mathcal{H}_B = \text{span}\{|b_1\rangle \cdots |b_N\rangle, \quad b_1, \dots, b_N \in \{0, 1\}\},$$

or, in the binary representation,

$$\mathcal{H}_B = \text{span}\left\{|b\rangle \mid b = \sum b_k 2^{k-1}, b \in \{0, 1, \dots, 2^N - 1\}\right\}.$$

In this basis, the bath Hamiltonian \hat{H}_B is a $2^N \times 2^N$ diagonal matrix:

$$\begin{aligned} (\hat{H}_B)_{bb'} &= \delta_{bb'} \mathcal{E}_b, \quad \mathcal{E}_b = \sum_k b_k E_k, \\ \text{for } b, b' &\in \{0, 1, \dots, 2^N - 1\}, \quad b_1, \dots, b_N \in \{0, 1\}. \end{aligned} \quad (20)$$

For future reference, let us call b_k the k -th digit of b . Now we are ready to calculate the correlation function $C_{ik, i'k'}(t-t')$. We have

$$\begin{aligned} C_{ik, i'k'}(t-t') &= \text{tr}_B \left(\frac{1}{Z_B} e^{-\beta \hat{H}_B} \hat{B}_{ik}(t) \hat{B}_{i'k'}(t') \right) \\ &= \frac{1}{Z_B} \sum_{b=0}^{2^N-1} e^{-\beta \mathcal{E}_b} \langle b | \hat{B}_{ik}(t) \hat{B}_{i'k'}(t') | b \rangle, \end{aligned} \quad (21)$$

where $Z_B = \sum_{b=0}^{2^N-1} e^{-\beta \mathcal{E}_b}$ is the normalizing factor. Using the resolution of identity $\mathbb{I} = \sum_{b'} |b'\rangle \langle b'|$, one can rewrite the correlation function as

$$\begin{aligned} C_{ik, i'k'}(t-t') &= \frac{1}{Z_B} \sum_{b=0}^{2^N-1} \sum_{b'=0}^{2^N-1} e^{-\beta \mathcal{E}_b} \langle b | \hat{B}_{ik}(t) | b' \rangle \langle b' | \hat{B}_{i'k'}(t') | b \rangle. \end{aligned} \quad (22)$$

Recall that $\hat{B}_{1k} = \hat{f}_{1k} = \hat{c}_k + \hat{c}_k^{\dagger}$, $\hat{B}_{2k} = \hat{f}_{2k} = i(\hat{c}_k - \hat{c}_k^{\dagger})$, and note that

$$\begin{aligned} \langle b | c_k(t) | b' \rangle &= \langle b | e^{\frac{i}{\varepsilon} \hat{H}_B t} c_k e^{-\frac{i}{\varepsilon} \hat{H}_B t} | b' \rangle \\ &= e^{\frac{i}{\varepsilon} (\mathcal{E}_b - \mathcal{E}_{b'}) t} \langle b | c_k | b' \rangle, \end{aligned} \quad (23)$$

Here we use $e^{-\frac{i}{\varepsilon} \hat{H}_B t} |b\rangle = e^{-\frac{i}{\varepsilon} \mathcal{E}_b t} |b\rangle$ according to Eq. (20). By definition of annihilation operators, $\langle b | c_k | b' \rangle$ is nonzero if and only if in the binary representation, $b_k = 0$, $b'_k = 1$, and except for the k -th digit, b and b' are the same. Similarly,

$$\begin{aligned} \langle b | c_k^{\dagger}(t) | b' \rangle &= \langle b | e^{\frac{i}{\varepsilon} \hat{H}_B t} c_k^{\dagger} e^{-\frac{i}{\varepsilon} \hat{H}_B t} | b' \rangle \\ &= e^{\frac{i}{\varepsilon} (\mathcal{E}_b - \mathcal{E}_{b'}) t} \langle b | c_k^{\dagger} | b' \rangle, \end{aligned} \quad (24)$$

where $\langle b | c_k^{\dagger} | b' \rangle$ is by definition nonzero if and only if in binary representation, $b_k = 1$, $b'_k = 0$, and except for the k -th digit, b and b' are the same.

In other words, given $b \in \{0, \dots, 2^N - 1\}$, there is a unique b' such that $\langle b | c_k(t) | b' \rangle$ ($\langle b | c_k^{\dagger}(t) | b' \rangle$) is nonzero if its k -th digit $b_k = 1$ ($b_k = 0$). This greatly simplifies the double sum in Eq. (22). We have

$$\begin{aligned} &\sum_{b=0}^{2^N-1} \sum_{b'=0}^{2^N-1} e^{-\beta \mathcal{E}_b} \langle b | c_k(t) | b' \rangle \langle b' | c_{k'}^{\dagger}(t') | b \rangle \\ &= \delta_{kk'} \sum_{\{b|b_k=0\}} e^{-\beta \mathcal{E}_b} e^{-\frac{i}{\varepsilon} E_k(t-t')}, \end{aligned} \quad (25)$$

$$\begin{aligned} &\sum_{b=0}^{2^N-1} \sum_{b'=0}^{2^N-1} e^{-\beta \mathcal{E}_b} \langle b | c_{k'}^{\dagger}(t) | b' \rangle \langle b' | c_k(t') | b \rangle \\ &= \delta_{kk'} \sum_{\{b|b_k=1\}} e^{-\beta \mathcal{E}_b} e^{\frac{i}{\varepsilon} E_k(t-t')}, \end{aligned} \quad (26)$$

Let

$$\begin{aligned} C_k^+(\tau) &= \frac{1}{Z_B} \sum_{\{b|b_k=0\}} e^{-\beta \mathcal{E}_b} e^{-\frac{i}{\varepsilon} E_k \tau}, \\ C_k^-(\tau) &= \frac{1}{Z_B} \sum_{\{b|b_k=1\}} e^{-\beta \mathcal{E}_b} e^{\frac{i}{\varepsilon} E_k \tau}, \end{aligned}$$

Combining Eqs. (22) to (24), we have

$$C_{ik, i'k'}(\tau) = \delta_{kk'} C_{ii', k}(\tau), \quad (27)$$

where

$$\begin{aligned}
C_{11,k}(\tau) &= C_k^+(\tau) + C_k^-(\tau), \\
C_{22,k}(\tau) &= C_k^+(\tau) + C_k^-(\tau), \\
C_{12,k}(\tau) &= -iC_k^+(\tau) + iC_k^-(\tau), \\
C_{21,k}(\tau) &= iC_k^+(\tau) - iC_k^-(\tau).
\end{aligned} \tag{28}$$

What's left to do is to calculate out $C_k^\pm(\tau)$. Note that

$$C_k^+(\tau) + C_k^-(\tau) = \frac{1}{Z_B} \sum_b e^{-\beta \mathcal{E}_b} e^{-\frac{i}{\varepsilon} E_k \tau} = e^{-\frac{i}{\varepsilon} E_k \tau},$$

$$\frac{C_k^+(\tau)}{C_k^-(\tau)} = \frac{\sum_{\{b|b_k=0\}} e^{-\beta \mathcal{E}_b} e^{-\frac{i}{\varepsilon} E_k (t-t')}}{\sum_{\{b|b_k=1\}} e^{-\beta \mathcal{E}_b} e^{-\frac{i}{\varepsilon} E_k (t-t')}} = e^{\beta E_k},$$

therefore we have

$$C_k^+(\tau) = \frac{\exp(-\frac{i}{\varepsilon} E_k \tau)}{1 + \exp(-\beta E_k)}, \quad C_k^-(\tau) = \frac{\exp(\frac{i}{\varepsilon} E_k \tau)}{1 + \exp(\beta E_k)}. \tag{29}$$

II.4. Towards the nMSSE model

Now we are ready to write down the nMSSE for the Anderson-Holstein model. Let us derive the formula in the spatial representation. The wavefunction has two components:

$$\Psi(x, t) = \begin{pmatrix} \psi_0(x, t) \\ \psi_1(x, t) \end{pmatrix}. \tag{30}$$

The first term on the right hand side of Eq. (17) is the system Hamiltonian itself:

$$\begin{aligned}
&\hat{H}_S \begin{pmatrix} \psi_0(x, t) \\ \psi_1(x, t) \end{pmatrix} \\
&= \begin{pmatrix} -\frac{\varepsilon^2}{2} \Delta + U_0(x) & \\ & -\frac{\varepsilon^2}{2} \Delta + U_1(x) \end{pmatrix} \begin{pmatrix} \psi_0(x, t) \\ \psi_1(x, t) \end{pmatrix}.
\end{aligned} \tag{31}$$

The second term is the stochastic noise, and could be rewritten as

$$\begin{aligned}
&\lambda \sum_{ik} \eta_{ik}(t) \hat{S}_{ik} \Psi(x, t) \\
&= \lambda \sum_k \left(\frac{i}{2} V_k(x) \eta_{1k}(t) \begin{pmatrix} i\psi_1 \\ -i\psi_0 \end{pmatrix} \right. \\
&\quad \left. - \frac{i}{2} V_k(x) \eta_{2k}(t) \begin{pmatrix} \psi_1 \\ \psi_0 \end{pmatrix} \right) \\
&= -\frac{i\lambda}{2} \sum_{k=1}^N V_k(x) (\eta_{2k}(t) \sigma_x + \eta_{1k}(t) \sigma_y) \begin{pmatrix} \psi_0(x, t) \\ \psi_1(x, t) \end{pmatrix},
\end{aligned} \tag{32}$$

and the stochastic noise η_{ik} satisfies that:

$$\begin{aligned}
\mathbb{E}(\eta_{ik}(t)) &= 0, \quad \mathbb{E}(\eta_{ik}(t) \eta_{i'k'}(t')) = 0, \\
\mathbb{E}(\eta_{ik}^*(t) \eta_{i'k'}(t')) &= \delta_{kk'} C_{ii',k}(t-t'), \quad i, i' = 1, 2.
\end{aligned} \tag{33}$$

The non-Markovian damping term is

$$-i \frac{\lambda^2}{\varepsilon} \int_0^t d\tau \sum_{ik, i'k'} C_{ik, i'k'}(\tau) \hat{S}_{ik} e^{-i\hat{H}_s \tau} \hat{S}_{i'k'} \psi(x, t - \tau).$$

Note that

$$e^{-\frac{i}{\varepsilon} \hat{H}_s \tau} = \begin{pmatrix} e^{-\frac{i}{\varepsilon} \hat{h}_0 \tau} & \\ & e^{-\frac{i}{\varepsilon} \hat{h}_1 \tau} \end{pmatrix} \tag{34}$$

With a straightforward calculation, we have

$$\begin{aligned}
&\sum_{i,j=1}^2 \sum_{k=1}^N C_{ij,k}(\tau) \hat{S}_{ik} e^{-\frac{i}{\varepsilon} \hat{H}_s \tau} \hat{S}_{jk} \psi(x, t - \tau) \\
&= -\sum_{k=1}^N \left(C_k^-(\tau) V_k(x) e^{-\frac{i}{\varepsilon} \hat{h}_1 \tau} V_k(x) \psi_0(x, t - \tau) \right. \\
&\quad \left. + C_k^+(\tau) V_k(x) e^{-\frac{i}{\varepsilon} \hat{h}_0 \tau} V_k(x) \psi_1(x, t - \tau) \right).
\end{aligned} \tag{35}$$

Here $\text{Diag} \begin{pmatrix} a \\ b \end{pmatrix}$ means $\begin{pmatrix} a & 0 \\ 0 & b \end{pmatrix}$. Note that operators $e^{-i\hat{h}_{0,1}\tau}$ and V_k typically does not commute.

Combining Eqs. (17), (31), (32) and (35), we arrive at the discretized nMSSE model for AH impurities:

$$\begin{aligned}
i\varepsilon \frac{\partial}{\partial t} \begin{pmatrix} \psi_0(x, t) \\ \psi_1(x, t) \end{pmatrix} &= \begin{pmatrix} \hat{h}_0 \psi_0(x, t) \\ \hat{h}_1 \psi_1(x, t) \end{pmatrix} \\
&- \frac{i\lambda}{2} \sum_{k=1}^N V_k(x) (\eta_{2k}(t) \sigma_x + \eta_{1k}(t) \sigma_y) \begin{pmatrix} \psi_0(x, t) \\ \psi_1(x, t) \end{pmatrix} \\
&+ i \frac{\lambda^2}{\varepsilon} \int_0^t d\tau \left(\sum_k C_k^-(\tau) V_k e^{-\frac{i}{\varepsilon} \hat{h}_1 \tau} V_k \psi_0(x, t - \tau) \right. \\
&\quad \left. + \sum_k C_k^+(\tau) V_k e^{-\frac{i}{\varepsilon} \hat{h}_0 \tau} V_k \psi_1(x, t - \tau) \right).
\end{aligned} \tag{36}$$

where $\hat{h}_{0,1} = -\frac{\varepsilon^2}{2} \Delta + U_{0,1}(x)$, and $\sigma_{x,y}$ is the Pauli matrices. Complex-valued Gaussian noise $\eta_{ik}(t)$ is defined in Eq. (33), and the memory kernel $C_k^\pm(\tau)$ is defined in Eq. (29).

II.5. Wide band limit and continuous band limit

In the wide band limit, the system-bath coupling $V(E, x)$ (or, in the discrete setting, $V_k(x)$) is considered to be independent of the metal spectrum E (or the discrete band index k), i.e. $V(\underline{E}, x) = V(x)$ for any $E \in [E_-, E_+]$, and $V_k(x) = \sqrt{\hbar_N} V(x)$. Let us define the total noise $\xi_i^{(N)}(t)$

$$\xi_i^{(N)}(t) = \sqrt{\hbar_N} \sum_{k=1}^N \eta_{ik}(t).$$

Recalling Eq. (33), we have

$$\begin{aligned} \mathbb{E}(\xi_i^{(N)}(t)) &= 0, \quad \mathbb{E}(\xi_i^{(N)}(t)\xi_{i'}^{(N)}(t')) = 0, \\ \mathbb{E}(\xi_i^{(N)*}(t)\xi_{i'}^{(N)}(t')) & \\ = h_N \sum_{kk'} \mathbb{E}(\eta_{ik}^*(t)\eta_{i'k'}(t')) &= h_N \sum_{k=1}^N C_{ii',k}(t-t'), \end{aligned} \quad (37)$$

For $i = 1, i' = 1$, we have

$$\begin{aligned} \mathbb{E}(\xi_1^{(N)*}(t)\xi_1^{(N)}(t')) &= h_N \sum_{k=1}^N C_{11,k}(t-t') \\ &= h_N \sum_{k=1}^N (C_k^+(t-t') + C_k^-(t-t')). \end{aligned}$$

Taking the continuous band limit, i.e. let $N \rightarrow \infty$, we have

$$\begin{aligned} h_N \sum_{k=1}^N C_k^\pm(\tau) &= h_N \sum_{k=1}^N \frac{\exp(\mp \frac{i}{\varepsilon} E_k \tau)}{1 + \exp(\mp \beta E_k)} \\ &\rightarrow \int_{E_-}^{E_+} \frac{\exp(\mp \frac{i}{\varepsilon} E \tau)}{1 + \exp(\mp \beta E)} dE =: c^\pm(\tau). \end{aligned}$$

For $(i, i') = (1, 2), (2, 1), (2, 2)$, things are similar. Therefore when $N \rightarrow \infty$, $\xi_i^{(N)}(t)$ converges to $\xi_i(t)$, which satisfies

$$\begin{aligned} \mathbb{E}(\xi_i(t)) &= 0, \quad \mathbb{E}(\xi_i(t)\xi_{i'}(t')) = 0, \quad i = 1, 2, \\ \mathbb{E}(\xi_1^*(t)\xi_1(t')) &= c^+(t-t') + c^-(t-t'), \\ \mathbb{E}(\xi_2^*(t)\xi_2(t')) &= c^+(t-t') + c^-(t-t'), \\ \mathbb{E}(\xi_1^*(t)\xi_2(t')) &= -ic^+(t-t') + ic^-(t-t'), \\ \mathbb{E}(\xi_2^*(t)\xi_1(t')) &= ic^+(t-t') - ic^-(t-t'). \end{aligned} \quad (38)$$

Now the noise term Eq. (32) becomes:

$$\begin{aligned} -\frac{i\lambda}{2} \sum_{k=1}^N V_k(x) (\eta_{2k}(t)\sigma_x + \eta_{1k}(t)\sigma_y) \begin{pmatrix} \psi_0(x, t) \\ \psi_1(x, t) \end{pmatrix} \\ \xrightarrow{N \rightarrow \infty} -\frac{i\lambda}{2} V(x) (\xi_2(t)\sigma_x + \xi_1(t)\sigma_y) \begin{pmatrix} \psi_0(x, t) \\ \psi_1(x, t) \end{pmatrix}. \end{aligned} \quad (39)$$

In the wide band limit and the continuous band limit, we also have

$$\begin{aligned} \sum_{k=1}^N C_k^\pm(\tau) V_k(x) e^{-\frac{i}{\varepsilon} \hat{h}_{0,1} \tau} V_k(x) \\ = \sum_{k=1}^N h_N C_k^\pm(\tau) V(x) e^{-\frac{i}{\varepsilon} \hat{h}_{0,1} \tau} V(x) \\ \rightarrow c^\pm(\tau) V(x) e^{-\frac{i}{\varepsilon} \hat{h}_{0,1} \tau} V(x). \end{aligned}$$

Therefore Eq. (35) becomes

$$-\begin{pmatrix} c^-(\tau) V(x) e^{-\frac{i}{\varepsilon} \hat{h}_1 \tau} V(x) \psi_0(x, t - \tau) \\ c^+(\tau) V(x) e^{-\frac{i}{\varepsilon} \hat{h}_0 \tau} V(x) \psi_1(x, t - \tau) \end{pmatrix}. \quad (40)$$

Replacing the noise and non-Markovian terms in Eq. (36) with Eqs. (39) and (40), we arrive at the nMSSE model in the wide and continuous band limit:

$$\begin{aligned} i\varepsilon \frac{\partial}{\partial t} \begin{pmatrix} \psi_0(x, t) \\ \psi_1(x, t) \end{pmatrix} &= \begin{pmatrix} \hat{h}_0 \psi_0(x, t) \\ \hat{h}_1 \psi_1(x, t) \end{pmatrix} \\ &- \frac{i\lambda V(x)}{2} (\xi_2(t)\sigma_x + \xi_1(t)\sigma_y) \begin{pmatrix} \psi_0(x, t) \\ \psi_1(x, t) \end{pmatrix} \\ &+ i \frac{\lambda^2}{\varepsilon} \int_0^t d\tau \begin{pmatrix} c^-(\tau) V(x) e^{-\frac{i}{\varepsilon} \hat{h}_1 \tau} V(x) \psi_0(x, t - \tau) \\ c^+(\tau) V(x) e^{-\frac{i}{\varepsilon} \hat{h}_0 \tau} V(x) \psi_1(x, t - \tau) \end{pmatrix}. \end{aligned} \quad (41)$$

The wide band limit still retained interesting physics since the separation of variables still preserves the spatial-inhomogeneity of the stochastic noise.

In the infinite temperature limit, i.e. $\beta = 0$, if $E_\pm = \pm\infty$, then the correlation function becomes

$$c^\pm(\tau) = \int_{-\infty}^{+\infty} \exp\left(\mp \frac{i}{\varepsilon} E \tau\right) d\tau = \pm 2\pi \varepsilon \delta(\tau). \quad (42)$$

III. FROM SSE TO QME

Quantum master equations (QME) are often used as semi-empirical models when studying open quantum systems such as metal surfaces [14, 48, 49]. Here we show that QME models of the Anderson-Holstein impurities are a second-step approximation to the SSE models in the interaction picture, and the well-known Redfield equation could be achieved with a further Markovian approximation.

III.1. Analytic derivation

In Eq. (41), we could think of the nMSSE effective Hamiltonian being $\hat{H}_S|\Psi\rangle + \hat{H}_{\text{int}}|\Psi\rangle$, where \hat{H}_{int} describes the effective interaction between the system and the bath:

$$\begin{aligned} \hat{H}_{\text{int}} \begin{pmatrix} \psi_0(x, t) \\ \psi_1(x, t) \end{pmatrix} \\ = -\frac{i\lambda V(x)}{2} (\xi_2(t)\sigma_x + \xi_1(t)\sigma_y) \begin{pmatrix} \psi_0(x, t) \\ \psi_1(x, t) \end{pmatrix} \\ + i \frac{\lambda^2}{\varepsilon} \int_0^t d\tau \begin{pmatrix} c^-(\tau) V(x) e^{-\frac{i}{\varepsilon} \hat{h}_1 \tau} V(x) \psi_0(x, t - \tau) \\ c^+(\tau) V(x) e^{-\frac{i}{\varepsilon} \hat{h}_0 \tau} V(x) \psi_1(x, t - \tau) \end{pmatrix} \\ = \left(\lambda \hat{H}_{\text{int}}^{(1)}(t) + \frac{\lambda^2}{\varepsilon} \hat{H}_{\text{int}}^{(2)}(t) \right) \begin{pmatrix} \psi_0(x, t) \\ \psi_1(x, t) \end{pmatrix}. \end{aligned} \quad (43)$$

Here we define $\hat{H}_{\text{int}}^{(1)}(t)$ and $\hat{H}_{\text{int}}^{(2)}(t)$ based on the order of λ .

Let $\Psi_I(x, t)$ be the wavefunction in the interaction picture. Then $\Psi_I(x, t)$ satisfies that:

$$i\varepsilon \frac{\partial}{\partial t} \Psi_I(x, t) = \hat{H}_{\text{int}, I}(t) \Psi_I(x, t), \quad (44)$$

where $\hat{H}_{\text{int},I}(t)$ is $\hat{H}_{\text{int}}(t)$ in the interaction picture:

$$\hat{H}_{\text{int},I}(t) = e^{\frac{i}{\varepsilon}\hat{H}_S t} \hat{H}_{\text{int}}(t) e^{-\frac{i}{\varepsilon}\hat{H}_S t}. \quad (45)$$

Note that we have the expansion $\hat{H}_{\text{int},I}(t) = \lambda \hat{H}_{\text{int},I}^{(1)}(t) + \frac{\lambda^2}{\varepsilon} \hat{H}_{\text{int},I}^{(2)}(t)$.

The quantum master equation describes the evolution of the expectation value of the density operator $\hat{\rho}_I = |\Psi_I\rangle\langle\Psi_I|$. If the wavefunction $|\Psi_I\rangle$ has the following asymptotic expansion:

$$|\Psi_I\rangle = |\Psi_I^{(0)}\rangle + \frac{\lambda}{\varepsilon} |\Psi_I^{(1)}\rangle + \left(\frac{\lambda}{\varepsilon}\right)^2 |\Psi_I^{(2)}\rangle + O\left(\left(\frac{\lambda}{\varepsilon}\right)^3\right),$$

then the expectation of the density matrix becomes

$$\begin{aligned} \mathbb{E}\hat{\rho}_I &= \mathbb{E}\hat{\rho}_I^{(0)} + \frac{\lambda}{\varepsilon} \mathbb{E}\hat{\rho}_I^{(1)} + \left(\frac{\lambda}{\varepsilon}\right)^2 \mathbb{E}\hat{\rho}_I^{(2)} + O\left(\left(\frac{\lambda}{\varepsilon}\right)^3\right), \\ \hat{\rho}_I^{(0)} &= |\Psi_I^{(0)}\rangle\langle\Psi_I^{(0)}|, \quad \hat{\rho}_I^{(1)} = |\Psi_I^{(0)}\rangle\langle\Psi_I^{(1)}| + |\Psi_I^{(1)}\rangle\langle\Psi_I^{(0)}|, \\ \hat{\rho}_I^{(2)} &= |\Psi_I^{(0)}\rangle\langle\Psi_I^{(2)}| + |\Psi_I^{(2)}\rangle\langle\Psi_I^{(0)}| + |\Psi_I^{(1)}\rangle\langle\Psi_I^{(1)}|. \end{aligned}$$

In the current work, ε is fixed, and considered to be $O(1)$.

Now we want to find $|\Psi_I^{(0)}\rangle, |\Psi_I^{(1)}\rangle, |\Psi_I^{(2)}\rangle$. Intergrating Eq. (44), and then substituting into itself, recalling that $\hat{H}_{\text{int},I}(t) = \lambda \hat{H}_{\text{int},I}^{(1)}(t) + \frac{\lambda^2}{\varepsilon} \hat{H}_{\text{int},I}^{(2)}(t)$ we have

$$\begin{aligned} \Psi_I(x, t) &= \Psi_I(x, 0) - \frac{i}{\varepsilon} \int_0^t \hat{H}_{\text{int},I}(t_1) \Psi_I(x, t_1) dt_1 \\ &= \Psi_I(x, 0) - \frac{i}{\varepsilon} \left(\int_0^t \hat{H}_{\text{int},I}(t_1) dt_1 \right) \Psi_I(x, 0) \\ &\quad + \left(-\frac{i}{\varepsilon} \right)^2 \int_0^t dt_1 \int_0^{t_1} dt_2 \hat{H}_{\text{int},I}(t_1) H_{\text{int},I}(t_2) \Psi_I(x, t_2) \\ &= \Psi_I(x, 0) - \frac{i}{\varepsilon} \lambda \left(\int_0^t \hat{H}_{\text{int},I}^{(1)}(t_1) dt_1 \right) \Psi_I(x, 0) \\ &\quad - \frac{i}{\varepsilon} \frac{\lambda^2}{\varepsilon} \left(\int_0^t \hat{H}_{\text{int},I}^{(2)}(t_1) dt_1 \right) \Psi_I(x, 0) \\ &\quad + \left(-\frac{i}{\varepsilon} \right)^2 \lambda^2 \int_0^t dt_1 \int_0^{t_1} dt_2 \hat{H}_{\text{int},I}^{(1)}(t_1) H_{\text{int},I}^{(1)}(t_2) \Psi_I^{(0)}(x, 0) \\ &\quad + O\left(\left(\frac{\lambda}{\varepsilon}\right)^3\right). \end{aligned} \quad (46)$$

Therefore we have

$$\begin{aligned} \Psi_I^{(0)}(x, t) &= \Psi_I(x, 0), \\ \Psi_I^{(1)}(x, t) &= -i \left(\int_0^t \hat{H}_{\text{int},I}^{(1)}(t_1) dt_1 \right) \Psi_I(x, 0), \\ \Psi_I^{(2)}(x, t) &= -i \left(\int_0^t \hat{H}_{\text{int},I}^{(2)}(t_1) dt_1 \right) \Psi_I(x, 0) \\ &\quad - \int_0^t dt_1 \int_0^{t_1} dt_2 \hat{H}_{\text{int},I}^{(1)}(t_1) H_{\text{int},I}^{(1)}(t_2) \Psi_I(x, 0). \end{aligned} \quad (47)$$

Note that $\mathbb{E}\Psi_I^{(1)}(x, t) = 0$ since the noise term has zero mean, therefore

$$\begin{aligned} \mathbb{E}\hat{\rho}_I^{(0)} &= \mathbb{E}\left(|\Psi_I^{(0)}\rangle\langle\Psi_I^{(0)}|\right) = |\Psi_I^{(0)}\rangle\langle\Psi_I^{(0)}|, \\ \mathbb{E}\hat{\rho}_I^{(1)} &= \mathbb{E}\left(|\Psi_I^{(0)}\rangle\langle\Psi_I^{(1)}| + |\Psi_I^{(1)}\rangle\langle\Psi_I^{(0)}|\right) \\ &= |\Psi_I^{(0)}\rangle\mathbb{E}\left(\langle\Psi_I^{(1)}|\right) + \mathbb{E}\left(|\Psi_I^{(1)}\rangle\right)\langle\Psi_I^{(0)}| = 0, \\ \mathbb{E}\hat{\rho}_I^{(2)} &= \mathbb{E}\left(|\Psi_I^{(0)}\rangle\langle\Psi_I^{(2)}| + |\Psi_I^{(2)}\rangle\langle\Psi_I^{(0)}| + |\Psi_I^{(1)}\rangle\langle\Psi_I^{(1)}|\right) \\ &= |\Psi_I^{(0)}\rangle\mathbb{E}\left(\langle\Psi_I^{(2)}|\right) + \mathbb{E}\left(|\Psi_I^{(2)}\rangle\right)\langle\Psi_I^{(0)}| \\ &\quad + \mathbb{E}\left(|\Psi_I^{(1)}\rangle\langle\Psi_I^{(1)}|\right). \end{aligned} \quad (48)$$

Let $\rho_I(t) = \mathbb{E}\hat{\rho}_I(t)$. With Eq. (48), we can differentiate $\rho_I(t)$ with respect to t and truncate terms that are higher than second order in λ , and then obtain the non-Markivian quantum master equation (nMQME):

$$\begin{aligned} \frac{d\rho_I(x, x', t)}{dt} &= \frac{\lambda^2}{\varepsilon^2} \left(\int_0^t \mathbf{c}_h(x, \tau) \rho_I(x, x', t - \tau) d\tau \right. \\ &\quad \left. + \int_0^t \mathbf{c}(x, x', \tau) \rho_I^{(d)}(x, x', t - \tau) d\tau + \text{h.c.} \right) + O\left(\left(\frac{\lambda}{\varepsilon}\right)^3\right) \\ \rho_I(0) &= \rho_0, \end{aligned} \quad (49)$$

where h.c. represents the Hermitian conjugate of the preceding terms, and

$$\begin{aligned} \mathbf{c}(x, x', \tau) &= \begin{pmatrix} c^+(\tau) V(x) V(x') & \\ & c^-(\tau) V(x) V(x') \end{pmatrix}, \\ \mathbf{c}_h(x, \tau) &= \begin{pmatrix} c^-(\tau) V(x) e^{-i\hat{h}_1 \tau} V(x) & \\ & c^+(\tau) V(x) e^{-i\hat{h}_0 \tau} V(x) \end{pmatrix}, \\ \rho_I^{(d)}(x, x', \tau) &= \begin{pmatrix} \rho_{I,11}(x, x', \tau) & \\ & \rho_{I,00}(x, x', \tau) \end{pmatrix}. \end{aligned}$$

For the detailed derivation of Eq. (49), which reduces to the further simplification of Eq. (48) and its derivative, please see Appendix A.

More generally, the above master equation could be derived starting with any initial time t_0 other than time $t_0 = 0$. In that case, the quantum master equation becomes

$$\begin{aligned} \frac{d\rho_I(x, x', t)}{dt} &= \frac{\lambda^2}{\varepsilon^2} \left(\int_0^{t-t_0} \mathbf{c}_h(x, \tau) \rho_I(x, x', t - \tau) d\tau \right. \\ &\quad \left. + \int_0^{t-t_0} \mathbf{c}(x, x', \tau) \rho_I^{(d)}(x, x', t - \tau) d\tau \right) + \text{h.c.}, \\ \rho_I(t_0) &= \rho_0. \end{aligned} \quad (50)$$

In Schrödinger picture, it becomes

$$\begin{aligned} \frac{d\rho(x, x', t)}{dt} &= -i \left(\hat{H}_s(x) - \hat{H}_s(x') \right) \rho(x, x', t) \\ &+ \frac{\lambda^2}{\varepsilon^2} e^{-i\hat{H}_S(x)(t-t_0)} e^{i\hat{H}_S(x')(t-t_0)} \times \left(\int_{t_0}^t d\tau \left(\mathbf{c}_h(x, t - \tau) e^{i\hat{H}_S(x)(\tau-t_0)} e^{-i\hat{H}_S(x')(\tau-t_0)} \rho(x, x', \tau) \right) \right. \\ &\left. + \int_{t_0}^t d\tau \left(\mathbf{c}(x, x', t - \tau) \sigma_x e^{i\hat{H}_S(x)(\tau-t_0)} e^{-i\hat{H}_S(x')(\tau-t_0)} \rho(x, x', \tau) \sigma_x + \text{h.c.} \right) \right), \end{aligned} \quad (51)$$

$$\rho(t_0) = \rho_I(t_0) = \rho_0.$$

Here $\sigma_x = \begin{pmatrix} 0 & 1 \\ 1 & 0 \end{pmatrix}$ as mentioned in Eq. (13).

III.2. Born-Markov approximation, finite-history Quantum Master Equation (FH-QME), Redfield equation, and their corresponding SSE

The non-Markovian quantum master equations Eq. (50) are mathematically complicated and computationally expensive. The widely-used Born-Markov approximation could be performed under the conditions that (1) the interaction between the system and the bath is weak, (2) the correlation time of the bath is much shorter than the characteristic time of the system. With the basic assumption $\rho_I(t - \tau) \approx \rho_I(t)$, the nMQME is reduced to

$$\begin{aligned} \frac{d\rho_I(x, x', t)}{dt} &= \frac{\lambda^2}{\varepsilon^2} \left(\int_0^{t-t_0} \mathbf{c}_h(x, \tau) d\tau \rho_I(x, x', t) \right. \\ &\left. + \int_0^{t-t_0} \mathbf{c}(x, x', \tau) d\tau \rho_I^{(d)}(x, x', t) \right) + \text{h.c.}, \end{aligned} \quad (52)$$

$$\rho_I(t_0) = \rho_0.$$

If t_0 is set to be 0, we refer to Eq. (52) as the finite-history QME (FH-QME). The corresponding SSE of FH-QME in the interaction picture could be easily obtained by modifying Eq. (43) with the approximation $\psi_{0,I}(x, t - \tau) \approx \psi_{0,I}(x, t)$ and $\psi_{1,I}(x, t - \tau) \approx \psi_{1,I}(x, t)$.

$$\begin{aligned} &i\varepsilon \frac{\partial}{\partial t} \begin{pmatrix} \psi_{0,I}(x, t) \\ \psi_{1,I}(x, t) \end{pmatrix} \\ &= -\frac{i\lambda V(x)}{2} (\xi_2(t)\sigma_x + \xi_1(t)\sigma_y) \begin{pmatrix} \psi_{0,I}(x, t) \\ \psi_{1,I}(x, t) \end{pmatrix} \\ &+ i\frac{\lambda^2}{\varepsilon} \int_0^t d\tau \begin{pmatrix} c^-(\tau)V(x)e^{-\frac{i}{\varepsilon}\hat{h}_1\tau}V(x)\psi_{0,I}(x, t) \\ c^+(\tau)V(x)e^{-\frac{i}{\varepsilon}\hat{h}_0\tau}V(x)\psi_{1,I}(x, t) \end{pmatrix} \end{aligned} \quad (53)$$

If we let $t_0 \rightarrow -\infty$ in Eq. (52), we obtain the infinite-history QME, also known as the Redfield equation:

$$\begin{aligned} \frac{d\rho_I(x, x', t)}{dt} &= \frac{\lambda^2}{\varepsilon^2} \left(\int_0^\infty \mathbf{c}_h(x, \tau) d\tau \rho_I(x, x', t) \right. \\ &\left. + \int_0^\infty \mathbf{c}(x, x', \tau) d\tau \rho_I^{(d)}(x, x', t) \right) + \text{h.c.}, \end{aligned} \quad (54)$$

$$\rho_I(-\infty) = \rho_0.$$

If we replace \int_0^t with $\int_{-\infty}^0$ in Eq. (53), we obtain the infinite-history SSE. The correspondence between SSE and QME, for example non-Markovian SSE (Eq. (41)) and non-Markovian QME (Eq. (49)), finite-history SSE (Eq. (53)) and finite-history QME (Eq. (52)), infinite-history SSE and Redfield equations (Eq. (54)) could be seen as the quantum analog of the relation between a stochastic process and its corresponding Fokker-Planck equation.

Since QME is obtained by neglecting higher order terms in the von-Neumann type equation of SSE, it should be viewed as a further approximation on top of SSE. In other words, we have established a hierarchy of models for Anderson-Holstein impurities, as detailed in Fig. 1. Going from SSE, to QME, and further to classical master equations (CME), one will make more assumptions and conduct more approximations. As a result, one would possibly lose crucial physical features while going along this hierarchy of approximations.

IV. NUMERICAL METHODS

IV.1. Noise Generation

To numerically simulate SSE, we need to generate stochastic noises that are subject to Eq. (38). The conventional noise generation scheme [47] relies on the analytic continuation of the correlation function to the complex plane. Such methods suffer from non-causality and non-physical artifacts due to the numerical instability of many rational approximation schemes [50, 51]. Here we present a stable noise generation scheme which do not rely on the interpolation of any correlation function.

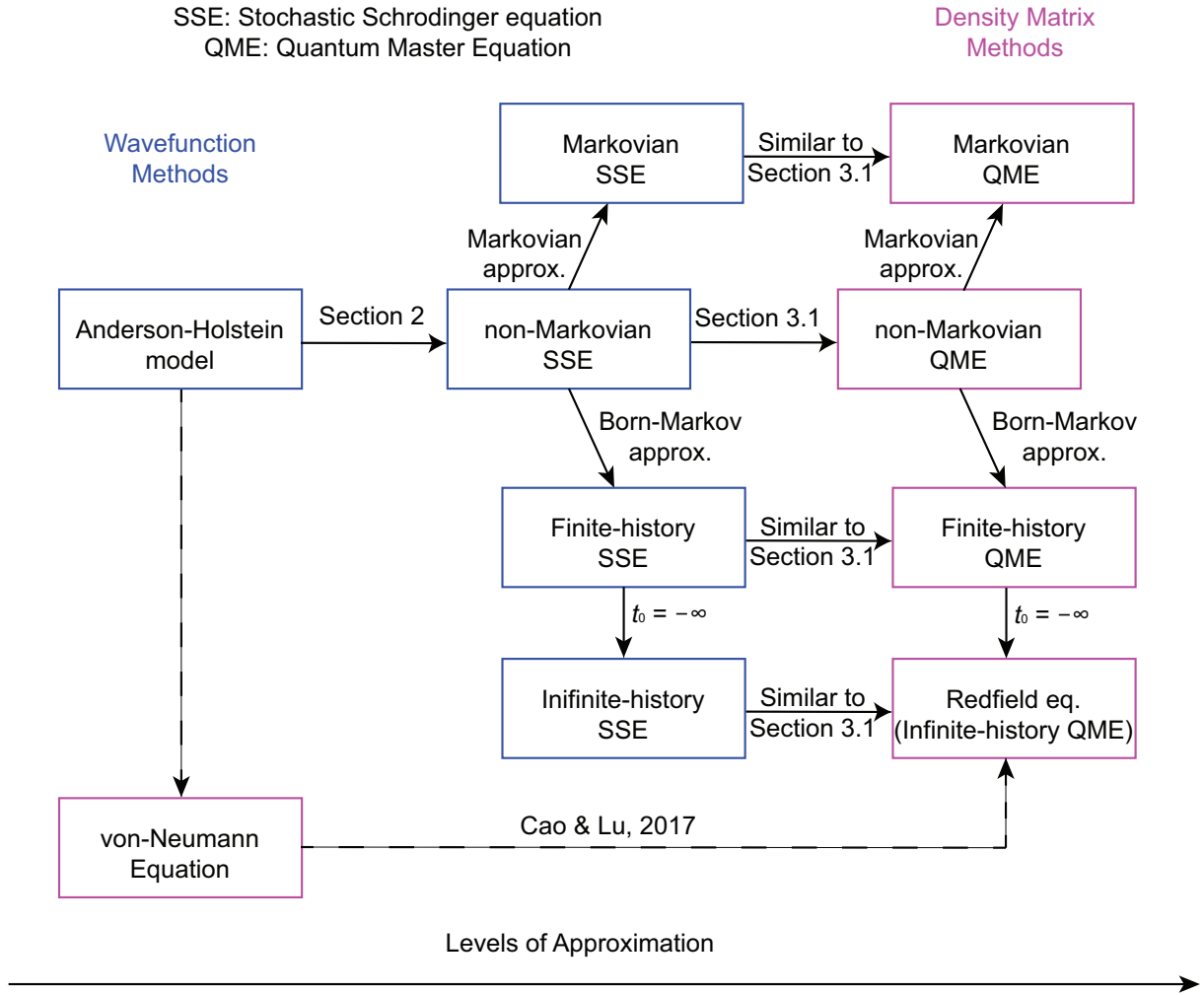


Figure 1. Hierarchy of various models for Anderson-Holstein impurities.

We first rewrite the noise term as follows:

$$\begin{aligned}
 & -\frac{i\lambda V(x)}{2} (\xi_2(t)\sigma_x + \xi_1(t)\sigma_y) \begin{pmatrix} \psi_0(x, t) \\ \psi_1(x, t) \end{pmatrix} \\
 & = \lambda V(x) \begin{pmatrix} \tilde{\xi}_+(t)\psi_1(x, t) \\ \tilde{\xi}_-(t)\psi_0(x, t) \end{pmatrix}, \\
 & \tilde{\xi}_+(t) = \frac{-\xi_1(t) - i\xi_2(t)}{2}, \quad \tilde{\xi}_-(t) = \frac{\xi_1(t) - i\xi_2(t)}{2}.
 \end{aligned} \tag{55}$$

where $\tilde{\xi}_\pm(t)$ satisfies that,

$$\begin{aligned}
 & \mathbb{E}(\tilde{\xi}_\pm(t)) = 0, \quad \mathbb{E}(\tilde{\xi}_+^*(t)\tilde{\xi}_-(t')) = 0, \\
 & \mathbb{E}(\tilde{\xi}_\pm(t)\tilde{\xi}_\pm(t')) = \mathbb{E}(\tilde{\xi}_\pm(t)\tilde{\xi}_\mp(t')) = 0, \\
 & \mathbb{E}(\tilde{\xi}_+^*(t)\tilde{\xi}_+(t')) = c^+(t-t'), \\
 & \mathbb{E}(\tilde{\xi}_-^*(t)\tilde{\xi}_-(t')) = c^-(t-t').
 \end{aligned} \tag{56}$$

In this way, $\tilde{\xi}_+(t)$ and $\tilde{\xi}_-(t)$ are decoupled, and could be generated separately. Let us define

$$W_\pm(t) = \int_0^t \tilde{\xi}_\pm(\tau) d\tau,$$

Then $W_\pm(t)$ is a Gaussian process with the covariance function $K(t, s)$:

$$K_\pm(s, t) = \int_0^s d\tau_1 \int_0^t d\tau_2 c^\pm(\tau_1 - \tau_2).$$

In particular, when $c^\pm(\tau_1 - \tau_2) = \delta(\tau_1 - \tau_2)$, we have $K_\pm(s, t) = \min(s, t)$, and $W_\pm(t)$ is the standard Brownian motion.

Generally, the sampling of $W_\pm(t)$ can be achieved by the Karhunen-Loève expansion. For a specified maximum time T_{\max} , consider the following eigenvalue problem:

$$\int_0^{T_{\max}} K_\pm(s, t) \phi_i^\pm(t) dt = \lambda_i^\pm \phi_i^\pm(s), \quad i = 1, 2, \dots \tag{57}$$

with the normalization condition $\int_0^{T_{\max}} \phi_i^\pm \phi_j^\pm dt = \delta_{ij}$. Then $W_\pm(t)$ has the Karhunen-Loève expansion

$$W_\pm(t) = \sum_{k=1}^{\infty} \alpha_k^\pm \sqrt{\lambda_k^\pm} \phi_k^\pm(t) \tag{58}$$

Here the $\alpha_k \sim N(0, 1)$ are i.i.d. random variables. In this way, the task of sampling the time-dependent noise is reduced to sampling scalar time-independent random variables. The eigenvalue problem Eq. (57) could be solved with a finite difference discretization in the time variable.

IV.2. Time evolution

We are solving Eq. (41) on the spatial domain $[a, b]$ and for time $[0, T]$. We use the following discretization:

$$\begin{aligned} \Delta x &= \frac{(b-a)}{M}, & \Delta t &= \frac{T}{N}. \\ x_j &:= a + j\Delta x, & j &= 0, 1, \dots, M-1, \\ t_n &:= n\Delta t, & n &= 0, 1, 2, \dots, N. \end{aligned} \quad (59)$$

To numerically solve Eq. (41), our strategy is as follows:

- For the system Hamiltonian \hat{H}_S , we use the Time Splitting Spectral method [52];
- For the fluctuation and dissipation terms, we use the Euler-Maruyama algorithm [53].

Let us present the numerical algorithm in detail for the Markovian SSE. With an efficient evaluation of the integration term, the strategy we described below is applicable to the non-Markovian case. In the Markovian limit, let $c_{\pm}(t)$ becomes $c_0^{\pm}\delta(t)$, where c_0^{\pm} are fixed constant. Then Eq. (41) becomes

$$\begin{aligned} & i\varepsilon \begin{pmatrix} d\psi_0(x, t) \\ d\psi_1(x, t) \end{pmatrix} \\ &= \begin{pmatrix} \hat{h}_0\psi_0(x, t) \\ \hat{h}_1\psi_1(x, t) \end{pmatrix} dt + \lambda V(x) \begin{pmatrix} \psi_1(x, t)dW_1(t) \\ \psi_0(x, t)dW_0(t) \end{pmatrix} \\ &+ \frac{i\lambda^2}{\varepsilon} |V(x)|^2 \begin{pmatrix} c_0^- \psi_0(x, t) \\ c_0^+ \psi_1(x, t) \end{pmatrix} dt, \quad x \in [a, b], \end{aligned} \quad (60)$$

Let us consider the following initial condition, which means that at $t = 0$ the molecule is neutral:

$$\begin{pmatrix} \psi_0(x, 0) \\ \psi_1(x, 0) \end{pmatrix} = \begin{pmatrix} \psi_0(x, 0) \\ 0 \end{pmatrix}.$$

Denote the numerical solution of $\psi_k(x_j, t_n)$, $k = 0, 1$ by $\psi_k^{j,n}$, $k = 0, 1$. From time $t = t_n$ to time $t = t_{n+1}$, we do the following:

1. Evolve using the potential term for a time step:

$$\begin{aligned} \psi_k^{j,*1} &= \exp\left(-i\frac{U_k(x_j)}{\varepsilon}\Delta t\right)\psi_k^{j,n}, \\ k &= 0, 1, \quad j = 0, \dots, M-1, \end{aligned} \quad (61)$$

2. Evolve using the kinetic term for a time step, but

in the frequency domain: for $k = 0, 1$, we have

$$\begin{cases} \{\widehat{\psi}_k^{l,*1}\}_{l=-\frac{M}{2}}^{\frac{M}{2}-1} = \text{FFT}\left(\{\psi_k^{j,*1}\}_{j=0}^{M-1}\right), \\ \widehat{\psi}_k^{l,*2} = \widehat{\psi}_k^{l,*1} \exp\left(-i\varepsilon\frac{\mu_l^2}{2}\Delta t\right), \quad l = -\frac{M}{2}, \dots, \frac{M}{2}-1, \\ \{\psi_k^{j,*2}\}_{j=0}^{M-1} = \text{iFFT}\left(\{\widehat{\psi}_k^{l,*2}\}_{l=-\frac{M}{2}}^{\frac{M}{2}-1}\right). \end{cases} \quad (62)$$

Here $\mu_l = \frac{2\pi l}{b-a}$, FFT and iFFT denote the Fast Fourier Transform and its inverse.

3. Deal with the fluctuation-dissipation term using the Euler-Maruyama scheme:

$$\begin{aligned} & \begin{pmatrix} \psi_0^{j,n+1} \\ \psi_1^{j,n+1} \end{pmatrix} \\ &= \begin{pmatrix} \psi_0^{j,*2} \\ \psi_1^{j,*2} \end{pmatrix} - i\frac{\lambda V(x_j)}{\varepsilon} \begin{pmatrix} (W_1(t_{n+1}) - W_1(t_n))\psi_1^{j,*2} \\ (W_0(t_{n+1}) - W_0(t_n))\psi_0^{j,*2} \end{pmatrix} \\ &+ \frac{\lambda^2}{\varepsilon^2} |V(x_j)|^2 \begin{pmatrix} c_0^- \psi_0^{j,*2} \\ c_0^+ \psi_1^{j,*2} \end{pmatrix} \Delta t. \end{aligned} \quad (63)$$

Remark 1. Here we use a first-order splitting scheme for the Hamiltonian part, which is sufficient for our problem. Higher-order splitting schemes also exist, such as Strang-Splitting and so on.

V. NUMERICAL RESULTS

The purpose of our numerical experiments is two-fold. On the one hand, we demonstrate that an ensemble of realizations of SSE could be used to obtain samples of physical observables of interest and thus directly manifest distributional information of these quantities, while QME could not provide a detailed characterization of the distribution except for moment information. On the other hand, we show that SSE and QME approaches indeed have the same thermodynamic equilibrium, while exhibiting different transient dynamics towards reaching such equilibrium.

V.1. Samples of physical observables by SSE

Let $x \in [a, b] = [-\pi, \pi]$, the maximal time $T = 10$. For simplicity, in this subsection, we choose the interaction strength $\lambda = \varepsilon$, which is neither necessary nor essential. Let us focus on the following system potentials which are harmonic with different centers:

$$U_0(x) = \frac{1}{2}x^2, \quad U_1(x) = \frac{1}{2}x^2 + 0.1x.$$

We aim to numerically explore SSE (60) in the wide band limit and with δ -correlated noise with special attention to investigating the role of the coupling potential $V(x)$. To this end, we consider the following examples:

Example 1. Propagating a Gaussian wavepacket with a bimodal coupling function:

$$\begin{aligned}\psi_0(x, 0) &= \frac{1}{(\pi\varepsilon)^{\frac{1}{4}}} \exp\left(\frac{-(x - q_0)^2}{2\varepsilon} + i\frac{p_0(x - q_0)}{\varepsilon}\right), \\ V(x) &= \exp(-10(x - 0.5)^2) + \exp(-40(x + 2)^2 - 1), \\ q_0 &= -1, p_0 = 0.5,\end{aligned}\tag{64}$$

Example 2. Propagating a Gaussian wavepacket with another bimodal coupling function:

$$\begin{aligned}\psi_0(x) &= \frac{1}{(\pi\varepsilon)^{\frac{1}{4}}} \exp\left(\frac{-(x - q_0)^2}{2\varepsilon} + i\frac{p_0(x - q_0)}{\varepsilon}\right), \\ V(x) &= 2 \exp(-10(x - 0.9)^2) + 5 \exp(-40(x + 0.5)^2), \\ q_0 &= -1, p_0 = 0.5.\end{aligned}\tag{65}$$

Example 3. Propagating a non-Gaussian wavepacket with a unimodal coupling function:

$$\begin{aligned}\psi_0(x) &\propto \exp\left(-5(x + 1)^2 + i\frac{\sin(x)}{\varepsilon}\right), \\ V(x) &= \exp(-10x^2).\end{aligned}\tag{66}$$

The coupling functions $V(x)$ that we considered are shown in Fig. 2. We remark that the experiments are designed such that either the wave packet is expected to exhibit decoherence through the interaction with the bath or is not initialized from a coherent state.

A typical trajectory of time evolution of SSE is shown in Fig. 3. We observe that the wave function is initially populated solely on level-0, it oscillates and propagates within a finite region due to the confinement of the harmonic potentials. In particular, only when it passes through an interaction region (where the coupling potential $V(x)$ is significant), it will partially and stochastically transmit to the other level. Thus the resulting dynamical behavior is rather complicated and the nonadiabatic phenomenon is nontrivial.

To explore the stochasticity of the SSE model, let us demonstrate with the numerical simulations of certain physical observables computed via an ensemble of realizations of SSE (60). We consider the transition rate $\langle R(t) \rangle$ and spatial average $\langle X(t) \rangle$, defined as:

$$\begin{aligned}\langle R(t) \rangle &= \frac{\int |\psi_0(x, t)|^2 dx}{\int (|\psi_0(x, t)|^2 + |\psi_1(x, t)|^2) dx}, \\ \langle X(t) \rangle &= \frac{\int x (|\psi_0(x, t)|^2 + |\psi_1(x, t)|^2) dx}{\int (|\psi_0(x, t)|^2 + |\psi_1(x, t)|^2) dx},\end{aligned}\tag{67}$$

We emphasize that $\langle \cdot \rangle$ mean taking the average over the quantum state, which is obtained by a one-time realization of SSE (60). Hence, $\langle R(t) \rangle$ and $\langle X(t) \rangle$ are random variables due to the stochasticity in the dynamics of (60). We repeat simulation (60) of each example for 4000 times, and the statistics (in the form of the histogram) of the observables are shown in Fig. 4, Fig. 5 and Fig. 6, respectively.

We can see that the coupling function $V(x)$ significantly affects the probability distribution of physical observables and SSE is capable of capturing both Gaussian and non-Gaussian distributional information of these quantities. Specifically, we have the following observations:

- (1) In Example 1, the coupling function $V(x)$ is bimodal: the primary coupling peak is placed near the center of the propagation region and the secondary coupling peak is placed near the boundary of the propagation region, where wave function turns its moving direction. We observe that the distribution of transition rate $\langle R(t) \rangle$ is non-Gaussian but the distribution of atomic position $\langle X(t) \rangle$ is Gaussian;
- (2) In Example 2, the coupling function $V(x)$ is also bimodal: both coupling peaks are near the center of the propagation region, but they are of different profiles. We observe that the distribution of transition rate $\langle R(t) \rangle$ is Gaussian but the distribution of atomic position $\langle X(t) \rangle$ is non-Gaussian;
- (3) In Example 3, although the wave function is initialized far from a coherent state, the coupling function $V(x)$ is unimodal, we have the distributions of transition rate $\langle R(t) \rangle$ and atomic position $\langle X(t) \rangle$ are both Gaussian.

While the results above are not conclusively definitive, this set of experiments already sheds light on the diverse stochastic behavior contained within the SSE models.

V.2. Comparison between SSE and QME

This part is devoted to a detailed comparison between SSE and QME models both in dynamics and equilibrium. Consider [14, 44, 48]

$$U_0(x) = \frac{1}{2}x^2, \quad U_1(x) = U_0(x) + \sqrt{2}gx + g^2 + E_d,\tag{68}$$

with the Markovian assumption $c^\pm(\tau) = c_0^\pm \delta(\tau)$, the corresponding QME of Eq. (49), transformed back to the Schrödinger picture, is

$$\begin{aligned}\frac{d\rho(t)}{dt} &= -\frac{i}{\varepsilon} \left[\hat{H}_S, \rho(t) \right] \\ &+ \frac{\lambda^2}{\varepsilon^2} |V|^2 \begin{pmatrix} 2(\rho_{00}(t) - \rho_{11}(t)) & \rho_{01}(t) + \rho_{10}(t) \\ \rho_{01}(t) + \rho_{10}(t) & 2(\rho_{11}(t) - \rho_{00}(t)) \end{pmatrix}.\end{aligned}\tag{69}$$

This is equivalent to the traditional Markovian QME

$$\begin{aligned}i\varepsilon \frac{d\rho(t)}{dt} &= \left[\begin{pmatrix} \hat{h}_0 & 0 \\ 0 & \hat{h}_1 \end{pmatrix}, \rho(t) \right] \\ &- i \frac{\lambda^2 V^2}{\varepsilon} \left[\hat{d} \hat{d}^\dagger \rho(t) - \hat{d}^\dagger \rho(t) \hat{d} + \rho(t) \hat{d}^\dagger \hat{d} - \hat{d} \rho(t) \hat{d}^\dagger + h.c. \right],\end{aligned}\tag{70}$$

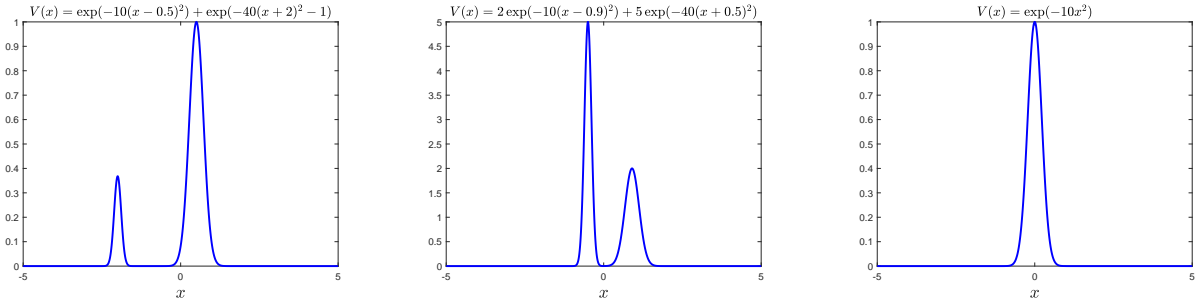
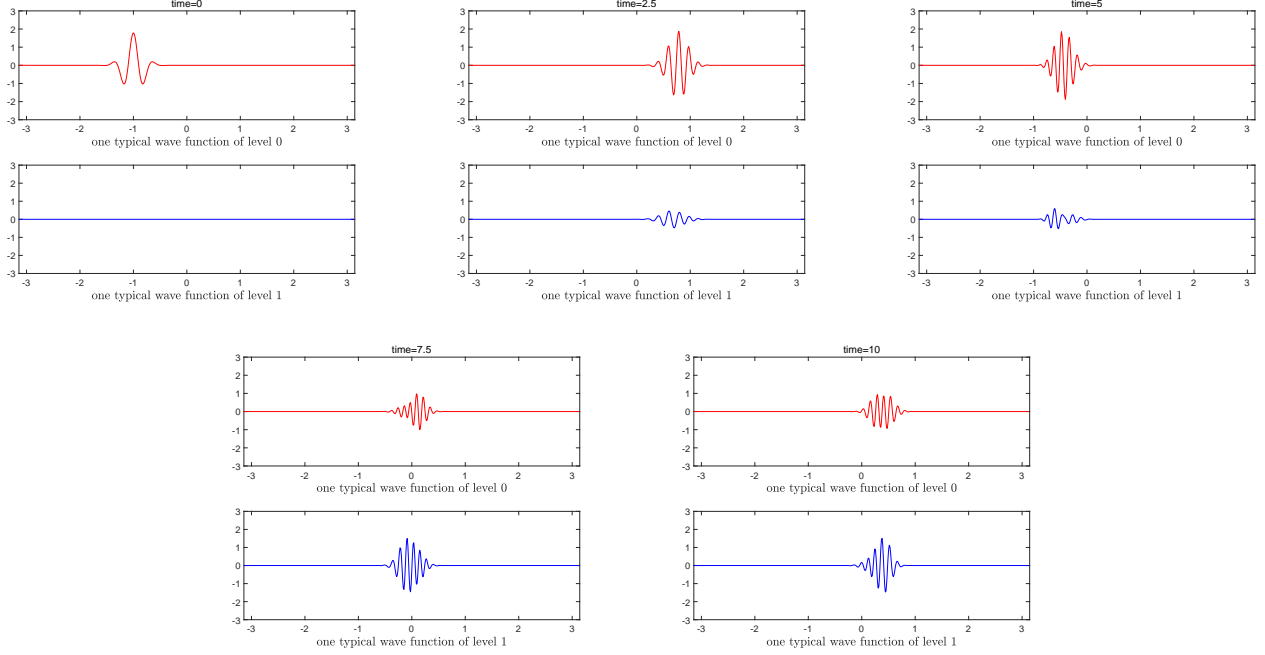
Figure 2. Plots of coupling functions $V(x)$ in example 1, 2 and 3.

Figure 3. The evolution of a typical wavefunction trajectory in example 1.

where \hat{d} and \hat{d}^\dagger are defined as in (4). We choose the following parameter:

$$L = 20, \quad g = 0.1, \quad E_d = 0.1, \quad V(x) = 1, \quad (71)$$

and the initial value

$$\psi_0(x, 0) \propto 1, \quad \rho(x, x', 0) = \psi_0(x, 0)\psi_0^*(x', 0).$$

In this example, we conduct the spatial discretization with Hermite polynomials. Also, note that the coupling function V is chosen to be spatially homogeneous, and the system is expected to reach the equilibrium.

Recall that the proposed models in this work are characterized by two parameters: the interaction strength λ and the semiclassical parameter ε . From the derivation of QME based on SSE, we can see that it holds when $\lambda \ll 1$ while ε is fixed, and a recent mathematical study reveals that QME can be directly derived only if $\lambda \ll \varepsilon$ [44]. In fact, our formulation facilitates more systematic

comparisons between SSE and QME with various combinations of λ and ε . The purpose of the following two numerical experiments is to compare the dynamics and steady states between SSE and QME under different ε versus λ relationships.

In the two numerical experiments, we test with two different $\varepsilon = 1/32$ and $1/64$. For each ε , we let the λ vary from ε to $\varepsilon/8$. The evolutions of the population of electrons on two levels based on SSE and QME for different ε and λ are shown in Fig. 7 and Fig. 8. The result indicates that (1) in this parameter setting, SSE and QME have the same equilibrium but different transient dynamics, and QME will reach the steady state faster than SSE; (2) for a fixed ε , λ only affects the relaxation time to reach the equilibrium, and a smaller λ indicates a longer relaxation time.

The former observation can be understood in two ways. Mathematically, the QME is not exactly equivalent to SSE, they are equal only if the higher-order term $O(\lambda^3)$

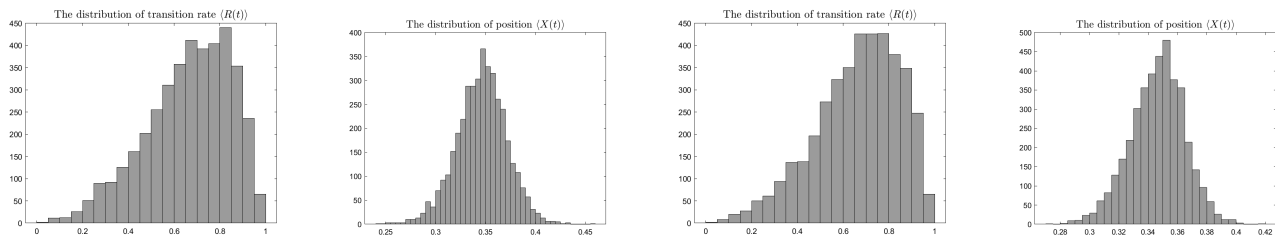


Figure 4. Histogram for transition rate and atomic position at $T = 10$, with $\varepsilon = 1/32$ and $\varepsilon = 1/64$, in example 1, from 4000 trajectories. The two subfigures on the left correspond to $\lambda = 1/32$ and the ones on the right correspond to $\lambda = 1/64$. This demonstrates a transition rate with a non-Gaussian distribution but an atomic position with a Gaussian-like distribution.

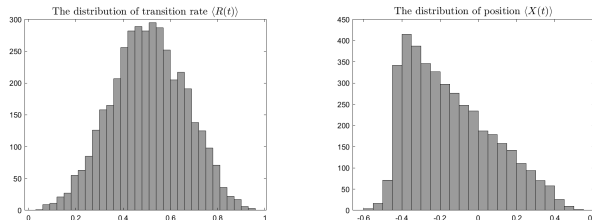


Figure 5. Histogram for transition rate and atomic position at $T = 10$, with $\varepsilon = 1/32$, in example 2, from 4000 trajectories. This demonstrates a transition rate with a Gaussian-like distribution but an atomic position with a non-Gaussian distribution.

is ignored. In a short time, the higher order terms lead to a difference in the dynamical behavior of the two, but in a long time, the higher order terms cancel each other out and thus have no effect on the steady state. Scientifically, QME is averaged over the stochastic term, such that the dissipation terms do not compete with the random fluctuations in dynamics, and thus the dynamics corresponding to QME will reach the steady state faster. This is a common relationship between SSE and QME and has been discussed in [54]. The latter shows that SSE still has the same steady state as QME when λ is not much less than ε , at least for a large class of parameter settings. This indicates that $\lambda \ll \varepsilon$ is only a sufficient condition, not a necessary one to establish qualitative connections between SSE and QME. More comparison studies and even qualitative connections are worth exploring in the future.

VI. CONCLUSION AND DISCUSSIONS

In this article, we propose a stochastic Schrödinger equation model for the Anderson-Holstein impurities, filling a gap in the study of open quantum systems with fermionic baths. The SSE model is obtained directly from the microscopic model instead of using empirical correlation functions. Through analytic derivations, we establish the theoretical relations between AH, SSE and QME, and introduce the hierarchy of modeling in Fig. 1. We also discuss efficient algorithms for noise generation

and sampling stochastic trajectories. Our numerical experiments show that SSE could be used to study physical observables and capture effects beyond the level of QME.

From the computational perspective, the non-Markovian term could be potentially expensive, especially in the high-dimensional case. If one is interested in the nonequilibrium dynamics of SSE, efficient algorithms that incorporate noise and treat the non-Markovian term with (quasi)-linear cost in time (for example, see [55]) would be required to propagate towards a longer time.

Our current studies focus on Holstein types of quantum impurities. Similar strategies are applicable to correlated systems via the pseudoparticle approach [56]. Understanding decoherence and relaxation dynamics of interacting systems [27, 57] will be the focus of our future work.

ACKNOWLEDGEMENT

Z.Z. is supported by the National Key R&D Program of China, Project Number 2021YFA1001200, and the NSFC, grant Number 12031013, 12171013. This work is partially supported by a grant from the Simons Foundation under Award No. 825053 (Z.H.). We thank helpful discussions with Dr. Yu Cao. L.X. thanks Dr. Hao Wu for his support and encouragement.

All authors contribute equally to this work.

[1] P. W. Anderson, *Physical Review* **124**, 41 (1961).

[2] R. Hanson, L. P. Kouwenhoven, J. R. Petta, S. Tarucha,

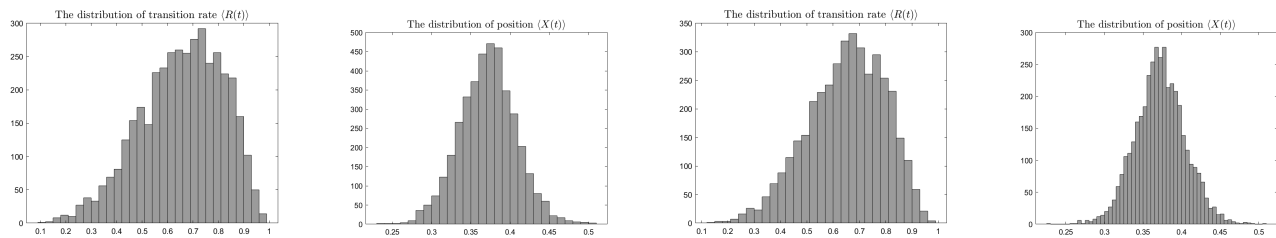


Figure 6. Histogram for transition rate and atomic position at $T = 10$, with $\varepsilon = 1/32$ and $\varepsilon = 1/64$, in example 3, from 4000 trajectories. The two subfigures on the left correspond to $\lambda = 1/32$ and the ones on the right correspond to $\lambda = 1/64$. This shows that the transition rate and atomic position both have a Gaussian-like distribution.

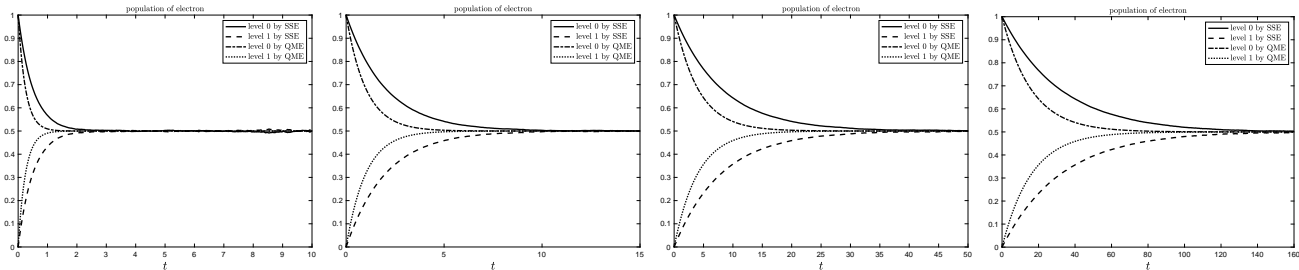


Figure 7. The population of electrons on two levels corresponding to $\varepsilon = 1/32$. From the top left to the bottom right, λ corresponds to $\varepsilon, \varepsilon/2, \varepsilon/4$, and $\varepsilon/8$, respectively. The sample size of SSE is $M = 80000$.

- and L. M. Vandersypen, *Reviews of modern physics* **79**, 1217 (2007).
- [3] R. Brako and D. Newns, *Journal of Physics C: Solid State Physics* **14**, 3065 (1981).
- [4] D. Newns, *Physical Review* **178**, 1123 (1969).
- [5] T. Holstein, *Annals of physics* **8**, 325 (1959).
- [6] B. Persson, *The Journal of Chemical Physics* **98**, 1659 (1993).
- [7] X. Luo, B. Jiang, J. I. Juaristi, M. Alducin, and H. Guo, *The Journal of Chemical Physics* **145**, 044704 (2016).
- [8] A. Nitzan and M. A. Ratner, *Science* **300**, 1384 (2003).
- [9] N. Shenvi, S. Roy, and J. C. Tully, *The Journal of chemical physics* **130**, 174107 (2009).
- [10] Z. Huang, L. Xu, and Z. Zhou, *Journal of Computational Physics* **474**, 111771 (2023).
- [11] G. Katz, Y. Zeiri, and R. Kosloff, *The Journal of Physical Chemistry B* **109**, 18876 (2005).
- [12] N. Shenvi, S. Roy, P. Parandekar, and J. Tully, *The Journal of chemical physics* **125** (2006).
- [13] D. C. Langreth and P. Nordlander, *Physical Review B* **43**, 2541 (1991).
- [14] W. Dou and J. E. Subotnik, *The Journal of chemical physics* **144**, 024116 (2016).
- [15] W. Ouyang, J. G. Saven, and J. E. Subotnik, *The Journal of Physical Chemistry C* **119**, 20833 (2015).
- [16] G. Miao, W. Ouyang, and J. Subotnik, *The Journal of Chemical Physics* **150** (2019).
- [17] S. Gao, *Physical review letters* **79**, 3101 (1997).
- [18] Y.-S. Wang, P. Nijjar, X. Zhou, D. I. Bondar, and O. V. Prezhdo, *The Journal of Physical Chemistry B* **124**, 4326 (2020).
- [19] S. Nakajima, *Progress of Theoretical Physics* **20**, 948 (1958).
- [20] T. P. Fay, *The Journal of Physical Chemistry Letters* **12**, 1407 (2021).
- [21] A. G. Redfield, in *Advances in Magnetic and Optical Resonance* (Elsevier, 1965), vol. 1, pp. 1–32.
- [22] A. S. Leathers and D. A. Micha, *The Journal of Physical Chemistry A* **110**, 749 (2006).
- [23] F. Elste, G. Weick, C. Timm, and F. von Oppen, *Applied Physics A* **93**, 345 (2008).
- [24] F. Elste, D. R. Reichman, and A. J. Millis, *Physical Review B* **81**, 205413 (2010).
- [25] F. Elste, D. R. Reichman, and A. J. Millis, *Physical Review B* **83**, 085415 (2011).
- [26] F. Elste, D. R. Reichman, and A. J. Millis, *Physical Review B* **83**, 245405 (2011).
- [27] R. Haertle, G. Cohen, D. Reichman, and A. Millis, *Physical Review B* **88**, 235426 (2013).
- [28] Y. Tanimura and R. Kubo, *Journal of the Physical Society of Japan* **58**, 101 (1989).
- [29] A. Erpenbeck and M. Thoss, *The Journal of Chemical Physics* **151** (2019).
- [30] P. Goetsch, P. Tombesi, and D. Vitali, *Physical Review A* **54**, 4519 (1996).
- [31] K. Shiokawa and B. Hu, *Physical Review E* **52**, 2497 (1995).
- [32] H. M. Wiseman, *Quantum and Semiclassical Optics: Journal of the European Optical Society Part B* **8**, 205 (1996).
- [33] J. Gambetta and H. M. Wiseman, *Physical Review A* **66**, 012108 (2002).
- [34] J. Gambetta and H. Wiseman, *Physical Review A* **68**, 062104 (2003).
- [35] H.-P. Breuer and F. Petruccione, *Physical Review E* **52**, 428 (1995).
- [36] H.-P. Breuer and J. Piilo, *Europhysics Letters* **85**, 50004 (2009).
- [37] X. Zhao, W. Shi, L.-A. Wu, and T. Yu, *Physical Review A* **86**, 032116 (2012).

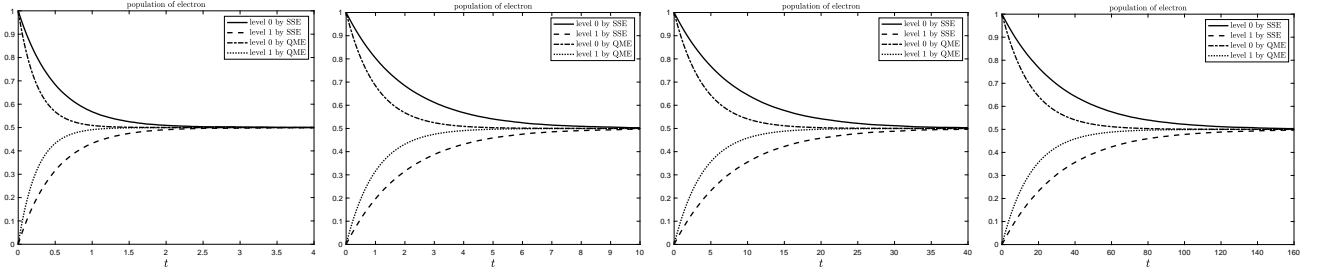


Figure 8. The population of electrons on two levels corresponding to $\varepsilon = 1/64$. From the top left to the bottom right, λ corresponds to $\varepsilon, \varepsilon/2, \varepsilon/4$, and $\varepsilon/8$, respectively. The sample size of SSE is $M = 80000$.

- [38] F. Nathan and M. S. Rudner, *Physical Review B* **102**, 115109 (2020).
- [39] H.-P. Breuer, F. Petruccione, et al., *The theory of open quantum systems* (Oxford University Press on Demand, 2002).
- [40] W. T. Strunz and T. Yu, *Physical Review A* **69**, 052115 (2004).
- [41] A. Jentzen and P. E. Kloeden, *Taylor approximations for stochastic partial differential equations* (SIAM, 2011).
- [42] Z. Zhang and G. Karniadakis, *Numerical methods for stochastic partial differential equations with white noise*, vol. 196 (Springer, 2017).
- [43] W. Shi, X. Zhao, and T. Yu, *Physical Review A* **87**, 052127 (2013).
- [44] Y. Cao and J. Lu, *Journal of Mathematical Physics* **58**, 122105 (2017), ISSN 0022-2488, 1089-7658, URL <http://aip.scitation.org/doi/10.1063/1.4993431>.
- [45] N. Bogoliubov, *J. Phys* **11**, 23 (1947).
- [46] N. Bogoljubov, V. V. Tolmachov, and D. Širkov, *Fortschritte der physik* **6**, 605 (1958).
- [47] P. Gaspard and M. Nagaoka, *The Journal of chemical physics* **111**, 5676 (1999).
- [48] W. Dou, A. Nitzan, and J. E. Subotnik, *The Journal of Chemical Physics* **142**, 084110 (2015), ISSN 0021-9606, 1089-7690, URL <http://aip.scitation.org/doi/10.1063/1.4908034>.
- [49] W. Dou, G. Miao, and J. E. Subotnik, *Physical Review Letters* **119**, 046001 (2017).
- [50] L. N. Trefethen, *Approximation Theory and Approximation Practice, Extended Edition* (SIAM, 2019).
- [51] Z. Huang, E. Gull, and L. Lin, *Physical Review B* **107**, 075151 (2023).
- [52] W. Bao, S. Jin, and P. A. Markowich, *Journal of Computational Physics* **175**, 487 (2002).
- [53] P. E. Kloeden, E. Platen, P. E. Kloeden, and E. Platen, *Stochastic differential equations* (Springer, 1992).
- [54] R. Biele and R. D'Agosta, *Journal of Physics: Condensed Matter* **24**, 273201 (2012).
- [55] J. Kaye and H. UR Strand, *Advances in Computational Mathematics* **49**, 63 (2023).
- [56] M. Eckstein and P. Werner, *Physical Review B* **82**, 115115 (2010).
- [57] R. Haertle and A. Millis, *Physical Review B* **90**, 245426 (2014).

Appendix A: Derivation of nMQME from nMSSE

We fill in the details of deriving the nMQME Eq. (49). Recall that from Eq. (47)

$$\Psi_I^{(2)}(x, t) = -i \left(\int_0^t \hat{H}_{\text{int}, I}^{(2)}(t_1) dt_1 \right) \Psi_I(x, 0) - \int_0^t dt_1 \int_0^{t_1} dt_2 \hat{H}_{\text{int}, I}^{(1)}(t_1) H_{\text{int}, I}^{(1)}(t_2) \Psi_I(x, 0).$$

Therefore

$$\mathbb{E} \left(\Psi_I^{(2)}(x, t) \right) = -i \left(\int_0^t \hat{H}_{\text{int}, I}^{(2)}(t_1) dt_1 \right) \Psi_I(x, 0) - \int_0^t dt_1 \int_0^{t_1} dt_2 \mathbb{E} \left(\hat{H}_{\text{int}, I}^{(1)}(t_1) H_{\text{int}, I}^{(1)}(t_2) \right) \Psi_I(x, 0). \quad (\text{A1})$$

Since $\mathbb{E}(\xi_i(t)\xi_{i'}(t')) = 0$, then

$$\begin{aligned} \mathbb{E} \left(\hat{H}_{\text{int}, I}^{(1)}(t_1) H_{\text{int}, I}^{(1)}(t_2) \right) &= -\frac{|V(x)|^2}{4} (\mathbb{E}(\xi_2(t_1)\xi_2(t_2))\mathbf{I} + \mathbb{E}(\xi_1(t_1)\xi_1(t_2))\mathbf{I} \\ &\quad + \mathbb{E}(\xi_2(t_1)\xi_1(t_2))\sigma_x\sigma_y + \mathbb{E}(\xi_1(t_1)\xi_2(t_2))\sigma_y\sigma_x) = 0. \end{aligned}$$

Therefore

$$\mathbb{E} \left(\Psi_I^{(2)}(x, t) \right) = -i \left(\int_0^t \hat{H}_{\text{int}, I}^{(2)}(t_1) dt_1 \right) \Psi_I(x, 0).$$

Taking derivatives with respect to t , we have

$$\begin{aligned} \frac{d}{dt} \mathbb{E} \left(\Psi_I^{(2)}(x, t) \right) &= -i \hat{H}_{\text{int}, I}^{(2)}(t) \Psi_I(x, 0) \\ &= \int_0^t d\tau \begin{pmatrix} c^-(\tau) V(x) e^{-i\hat{h}_1 \tau} V(x) & \\ & c^+(\tau) V(x) e^{-i\hat{h}_0 \tau} V(x) \end{pmatrix} \begin{pmatrix} \psi_0(x, t - \tau) \\ \psi_1(x, t - \tau) \end{pmatrix} \\ &= \int_0^t d\tau \begin{pmatrix} c^-(\tau) V(x) e^{-i\hat{h}_1 \tau} V(x) & \\ & c^+(\tau) V(x) e^{-i\hat{h}_0 \tau} V(x) \end{pmatrix} \begin{pmatrix} \psi_0(x, 0) \\ \psi_1(x, 0) \end{pmatrix} + O(\lambda). \end{aligned}$$

Another ingredient we need is $\mathbb{E} \left(|\Psi_I^{(1)}\rangle \langle \Psi_I^{(1)}| \right)$. Again recall from Eq. (47) that

$$\Psi_I^{(1)}(x, t) = -\frac{V(x)}{2} \left(\int_0^t (\xi_2(t_1) \sigma_x + \xi_1(t_1) \sigma_y) dt_1 \right) \Psi_I(x, 0).$$

Then

$$\begin{aligned} \mathbb{E} \left(\langle x | \Psi_I^{(1)} \rangle \langle \Psi_I^{(1)} | x' \rangle \right) &= \frac{V(x)V(x')}{4} \int_0^t \int_0^t \sigma_x \hat{\rho}_I^{(0)}(x, x') \sigma_x \mathbb{E} (\xi_2(t_1) \xi_2^*(t_2)) + \sigma_y \hat{\rho}_I^{(0)}(x, x') \sigma_y \mathbb{E} (\xi_1(t_1) \xi_1^*(t_2)) \\ &\quad + \sigma_y \hat{\rho}_I^{(0)}(x, x') \sigma_x \mathbb{E} (\xi_1(t_1) \xi_2^*(t_2)) + \sigma_x \hat{\rho}_I^{(0)}(x, x') \sigma_y \mathbb{E} (\xi_2(t_1) \xi_1^*(t_2)) dt_1 dt_2 \end{aligned}$$

Further simplifications give us

$$\mathbb{E} \left(\langle x | \Psi_I^{(1)} \rangle \langle \Psi_I^{(1)} | x' \rangle \right) = V(x)V(x') \int_0^t \int_0^t \begin{pmatrix} \rho_{I,11}^{(0)}(x, x') c^+(t_2 - t_1) & \\ & \rho_{I,00}^{(0)}(x, x') c^-(t_2 - t_1) \end{pmatrix} dt_1 dt_2$$

Now we are ready to derive the master equation. Since $\rho_I(t) = \mathbb{E} \hat{\rho}_I(t)$, $\mathbb{E} \hat{\rho}_I^{(0)}$ is a fixed value, $\mathbb{E} \hat{\rho}_I^{(1)} = 0$, therefore $\frac{d\rho_I(t)}{dt} = \frac{\lambda^2}{\varepsilon^2} \frac{d}{dt} \mathbb{E} \hat{\rho}_I^{(2)}(t) + O(\lambda^3)$. We have

$$\begin{aligned} \frac{d\rho_I(x, x', t)}{dt} &= \frac{\lambda^2}{\varepsilon^2} \left(\langle x | \Psi_I^{(0)} \rangle \frac{d}{dt} \mathbb{E} \left(\langle \Psi_I^{(2)} | x' \rangle \right) + \frac{d}{dt} \mathbb{E} \left(\langle x | \Psi_I^{(2)} \rangle \right) \langle \Psi_I^{(0)} | x' \rangle + \frac{d}{dt} \mathbb{E} \left(\langle x | \Psi_I^{(1)} \rangle \langle \Psi_I^{(1)} | x' \rangle \right) \right) + O(\lambda^3) \\ &= \frac{\lambda^2}{\varepsilon^2} \left(\int_0^t d\tau \begin{pmatrix} c^-(\tau) V(x) e^{-i\hat{h}_1 \tau} V(x) & \\ & c^+(\tau) V(x) e^{-i\hat{h}_0 \tau} V(x) \end{pmatrix} \rho_I^{(0)}(x, x') \right. \\ &\quad \left. + \int_0^t V(x)V(x') \begin{pmatrix} \rho_{I,11}^{(0)}(x, x') c^+(t - \tau) & \\ & \rho_{I,00}^{(0)}(x, x') c^-(t - \tau) \end{pmatrix} d\tau \right) + h.c. + O(\lambda^3) \\ &= \frac{\lambda^2}{\varepsilon^2} \left(\int_0^t d\tau \begin{pmatrix} c^-(\tau) V(x) e^{-i\hat{h}_1 \tau} V(x) & \\ & c^+(\tau) V(x) e^{-i\hat{h}_0 \tau} V(x) \end{pmatrix} \rho_I(x, x', t - \tau) \right. \\ &\quad \left. + \int_0^t V(x)V(x') \begin{pmatrix} \rho_{I,11}(x, x', \tau) c^+(t - \tau) & \\ & \rho_{I,00}(x, x', \tau) c^-(t - \tau) \end{pmatrix} d\tau \right) + h.c. + O(\lambda^3). \end{aligned}$$